Received: 11 June 2019 | Revised: 2 September 2019 | Accepted: 3 September 2019

DOI: 10.1002/cne.24773

RESEARCH ARTICLE

JCN RESEARCH IN SYSTEMS NEUROSCIENCE THE JOURNAL OF COMPARATIVE NEUROLOGY WILEY

Differential expression of secretagogin immunostaining in the hippocampal formation and the entorhinal and perirhinal cortices of humans, rats, and mice

Silvia Tapia-González[1,2,3] | Ricardo Insausti[4] | Javier DeFelipe[1,2,3]

[1]Laboratorio Cajal de Circuitos Corticales, Centro de Tecnología Biomédica, Universidad Politécnica de Madrid, Madrid, Spain

[2]Instituto Cajal, Consejo Superior de Investigaciones Científicas (CSIC), Madrid, Spain

[3]Centro de Investigación Biomédica en Red sobre Enfermedades Neurodegenerativas (CIBERNED), ISCIII, Madrid, Spain

[4]Laboratorio de Neuroanatomía Humana, Facultad de Medicina, Universidad de Castilla-La Mancha, Albacete, Spain

Correspondence
Javier DeFelipe, Laboratorio Cajal de Circuitos Corticales, Centro de Tecnología Biomédica, Universidad Politécnica de Madrid, Campus Montegancedo S/N, Pozuelo de Alarcon, 28223 Madrid, and Instituto Cajal (CSIC), Avenida Doctor Arce, 37, 28002 Madrid, Spain.
Email: defelipe@cajal.csic.es

Funding information
Centro de Investigación en Red sobre Enfermedades Neurodegenerativas, Grant/Award Number: CB06/05/0066; European Union's Horizon 2020 Research and Innovation Programme (Human Brain Project), Grant/Award Number: 785907; Ministerio de Ciencia, Innovación y Universidades, Grant/Award Number: PGC2018-094307-B-I00

Peer Review
The peer review history for this article is available at https://publons.com/publon/10.1002/cne.24773.

Abstract

Secretagogin (SCGN) is a recently discovered calcium-binding protein belonging to the group of EF-hand calcium-binding proteins. SCGN immunostaining has been described in various regions of the human, rat and mouse brain. In these studies, it has been reported that, in general, the patterns of SCGN staining differ between rodents and human brains. These differences have been interpreted as uncovering phylogenetic differences in SCGN expression. Nevertheless, an important aspect that is not usually taken into account is that different methods are used for obtaining and processing brain tissue coming from humans and experimental animals. This is a critical issue since it has been shown that post-mortem time delay and the method of fixation (i.e., perfused vs. nonperfused brains) may influence the results of the immunostaining. Thus, it is not clear whether differences found in comparative studies with the human brain are simply due to technical factors or species-specific differences. In the present study, we analyzed the pattern of SCGN immunostaining in the adult human hippocampal formation (DG, CA1, CA2, CA3, subiculum, presubiculum, and parasubiculum) as well as in the entorhinal and perirhinal cortices. This pattern of immunostaining was compared with rat and mouse that were fixed either by perfusion or immersion and with different post-mortem time delays (up to 5 hr) to mimic the way the human brain tissue is usually processed. We found a number of clear similarities and differences in the pattern of labeling among the human, rat, and mouse in these brain regions as well as between the different brain regions examined within each species. These differences were not due to the fixation.

KEYWORDS
comparative studies, entorhinal cortex, hippocampal formation, human, rat and mouse brains, immunostaining, perirhinal cortex, post-mortem, RRID:AB_1079874, RRID:AB_10807945, secretagogin

1 | INTRODUCTION

Secretagogin (SCGN) is a recently discovered calcium-binding protein belonging to the group of EF-hand Ca^{2+}-binding proteins (Archer & Wagner, 2000). As reported by Wagner et al. (2000), sequence analysis shows that SCGN has six Ca^{2+}-binding loops with typical EF-hand tandem repeats and has marked homology to the Ca^{2+}-binding proteins calbindin D-28k and calretinin, which also have six EF-hand motifs.

However, the distribution in the brain of calbindin D-28k-, calretinin-, and SCGN-immunoreactive (-ir) neurons and neuropil immunostaining is different (e.g., Arellano, Munoz, Ballesteros-Yanez, Sola, & DeFelipe, 2004; Barinka et al., 2012; Cho et al., 2011; Miettinen, Pitkanen, & Miettinen, 1997; Seress et al., 1993; Wouterlood, van Denderen, van Haeften, & Witter, 2000). SCGN has been less intensively studied (particularly in the human brain) than the other calcium-binding proteins, but it has been described in various regions of the human, rat, and mouse brain (e.g., Gartner et al., 2001; Kosaka & Kosaka, 2013; Mulder, Bjorling, et al., 2009; Mulder et al., 2010; Mulder, Zilberter, et al., 2009; Wagner et al., 2000).

These studies reported that, in general, the patterns of SCGN-immunoreactivity differ between rodents and human brains, although few detailed comparative studies have been carried out. It seems that SCGN labeling identifies certain neuronal subtypes and might be used as a marker to delineate particular brain structures, as well as to identify hierarchical organizing principles. Therefore, the study of SCGN-immunoreactivity in the brain is of great interest. For example, in a recent study in the mouse brainstem, few SCGN-ir cells were found, whereas numerous SCGN-ir neurons were observed in the rat brainstem (Kosaka & Kosaka, 2018). Another study reported that a subpopulation of parvalbumin immunoreactive interneurons coexpressed SCGN in the dorsal striatum of rats, but not in mice (Garas et al., 2016). Furthermore, it has been shown that SCGN is expressed by cholinergic neurons in embryonic basal forebrain and neuroblasts in the rostral migratory stream in gray mouse lemurs, but not in mice. There are also differences in SCGN immunostaining during development in the granule cell layer of the dentate gyrus (DG) and pyramidal cell layer of CA1–CA3 fields between gray mouse lemurs and mice (Mulder et al., 2010; Mulder, Zilberter, et al., 2009). These differences have been interpreted by Mulder et al. as uncovering phylogenetic differences in SCGN expression. More recently, it has also been reported that SCGN is expressed by developing neocortical GABAergic neurons in humans but not in mice (Raju, Spatazza, Stanco, Sorrells, & Kelley, 2017). In the human brain, SCGN immunostaining has been described in both cerebellar basket and stellate cells and in neurons of temporal, frontal, hippocampal, and hypothalamic regions (Gartner et al., 2001). In addition, Attems et al. (2007) reported that SCGN-immunoreactivity in the human hippocampus was restricted to a subset of pyramidal neurons in subiculum, CA1, CA2, CA3, and CA4 and that these cells were mostly unaffected by tau pathology in patients with Alzheimer's disease (Attems et al., 2008).

Nevertheless, an important aspect that is not usually taken into account is that different methods are used for obtaining and processing brain tissue coming from humans and experimental animals. Indeed, it has been shown that post-mortem time (PT) delay and the method of fixation (i.e., perfused vs. nonperfused brains) may influence the results of the immunostaining (e.g., see Gonzalez-Riano et al., 2017; Lavenex, Lavenex, Bennett, & Amaral, 2009). Thus, it is not clear whether differences found in comparative studies with the human brain are simply due to technical factors or species-specific differences. In the present study, we analyzed the pattern of SCGN immunostaining in the adult human hippocampal formation compared with rat and mouse that were fixed either by perfusion or immersion and with different PT delays (up to 5 hr) to mimic the way that the human brain tissue is usually processed. We focused on the characterization of the pattern of SCGN-immunoreativity in different hippocampal fields (DG, CA1, CA2, CA3, subiculum, presubiculum, and parasubiculum) as well as in the entorhinal (EC) and perirhinal (PRC) cortices of the three species. We found a number of clear similarities and differences in the pattern of labeling among the human, rat, and mouse in these brain regions as well as between the different brain regions examined within each species. These differences were not due to the fixation.

2 | MATERIALS AND METHODS

2.1 | Humans

Human brain tissue was obtained at autopsy from the Unidad Asociada Neuromax—Laboratorio de Neuroanatomía Humana, Facultad de Medicina, Universidad de Castilla-La Mancha, Albacete, and the Laboratorio Cajal de Circuitos Corticales UPM-CSIC, Madrid, Spain. The tissue was obtained following national laws and international ethical and technical guidelines on the use of human samples for biomedical research purposes. In this study, we used samples of human brain tissue from 3 control human brains (subjects with no recorded neurological or psychiatric alterations): 2 males, aged 45 (AB1) and 53 (AB3) and 1 female, aged 53 (AB2). The PT between death and brain fixation varied between 1.5 and 4 hr (AB1: 1.5 hr; AB3: 3.5 hr; and AB2: 4 hr PT). Tissue from human brain AB1 and AB2 has been used in a previous study (Anton-Fernandez, Aparicio-Torres, Tapia, DeFelipe, & Munoz, 2017). The cause of death was pleural mesothelioma (case AB1), septic shock of pulmonary origin (case AB2), and metastatic bladder carcinoma (case AB3). Upon removal, the brains (AB2, AB3) were immediately fixed in cold 4% paraformaldehyde (PFA) in 0.1 mol/L, pH 7.4 phosphate buffer (PB), and sectioned into 1.5 cm-thick coronal slabs. The hippocampus was cut into 1 cm blocks and post-fixed in the same fixative for 24–48 hr at 4°C. Case AB1 was perfused through both internal carotid arteries <1 hr after death with a saline solution followed by 4% PFA in PB. The brain was then removed and post-fixed as described above. The tissue blocks were then cryoprotected in 25% sucrose in PB and stored at −20°C in a solution of glycerol, ethylene glycol and PB. Serial hippocampal sections (50 μm) of each case were obtained using a vibratome (Leica VT2100S St. Louis, MO), and processed for histochemical and immunohistochemical experiments. The sections immediately adjacent to those stained immunohistochemically were Nissl-stained in order to identify the hippocampal fields and the laminar boundaries.

2.2 | Animals

This study was performed in 2-month-old male C57BL/6 J mice and 3-month-old male Wistar albino male rats (Charles River Laboratories, Wilmington, MA). Animals were kept in a 12:12-hr light/dark cycle and received food and water ad libitum. All experimental protocols involving the use of animals were performed in accordance with

recommendations for the proper care and use of laboratory animals, and under the authorization of the regulations and policies governing the care and use of laboratory animals (EU directive no. 86/609 and Council of Europe Convention ETS1 23, EU decree 2001-486 and Statement of Compliance with Standards for Use of Laboratory Animals by Foreign Institutions no. A5388-01, National Institutes of Health [USA]). Special care was taken to minimize animal suffering and to reduce the number of animals used to the minimum required for this study.

In order to perform comparative studies between human and rodent species in the present study, we analyzed SCGN-ir in two groups: one group of mice (n = 4) and another of rats (n = 6). All animals were anesthetized with a pentobarbital lethal injection (40 mg/kg BW, Vetoquinol, Madrid, Spain) and transcardially perfused with a saline solution followed by 4% PFA in PB. The brains were removed from the skull and post-fixed by immersion in the same fixative for 20 hr at 4°C.

Furthermore, we tested the possible effects of 2 and 5 hr PT on SCGN immunostaining in two groups of rats and two of mice. Rats and mice were sacrificed with the same pentobarbital lethal injection as described above. Thereafter, their brains were removed at 2 and 5 hr PT (n = 2 rats and n = 2 mice, for each time point) as described in our previous study (Gonzalez-Riano et al., 2017), and fixed in PB-buffered 4% PFA overnight (20 hr) at 4°C.

After rinsing in PB, the brain tissue from the six groups of animals was cut into 50-μm-thick, coronal slices using a vibratome (Leica VT2100S, St. Louis, MO). The brain tissue was processed as described above and then processed for immunohistochemistry.

2.3 | Immunohistochemistry

The rabbit anti-SCGN antibody (RRID:AB_1079874) used in the present study was obtained from Sigma-Aldrich (see below). This antibody was raised against recombinant human SCGN and has been described, characterized and tested in detail for its specificity by Mulder et al. (Mulder, Zilberter, et al., 2009, Mulder, Bjorling, et al., 2009, Mulder et al., 2010, see also Ellis et al., 2019). Using immunohistochemical techniques with this antibody, SCGN has been detected in the brain of various mammalian species including rat (Mulder, Bjorling, et al., 2009), mouse and mouse lemur (Mulder et al., 2010; Mulder, Zilberter, et al., 2009), ferret (Ellis et al., 2019), and human (Raju et al., 2017). This anti-SCGN antibody has also been characterized by performing western blot analysis, yielding a single protein band of ~32 kDa in BRIN-BD11 insulinoma cell lysates (Sanagavarapu, Weiffert, Ni Mhurchu, O'Connell, & Linse, 2016), rat brain homogenates (Mulder, Bjorling, et al., 2009), extracts of different brain areas from mouse brain (Mulder et al., 2010; Mulder, Zilberter, et al., 2009), and ferret whole brain lysates (Ellis et al., 2019). The rabbit anti-NeuN antibody (RRID:AB_10807945) employed in the present study was obtained from Millipore (see below). It was characterized by the manufacturer by performing immunohistochemistry techniques in human (cerebellum and cerebral cortex) and mouse (hippocampus) brain tissue sections, as well as western blot analyses in mouse and rat brain tissue lysates, observing 2–3 bands in the 46–48 kDa range. Immunohistochemical experiments were carried out in free-floating sections under moderate shaking. The endogenous peroxidase activity was quenched in a solution of 1.66% hydrogen peroxide in 50% ethanol in PB for 30 min at room temperature. After several washes in 0.1 M phosphate buffer (pH 7.4) containing 0.3% TritonX-100 (washing buffer), sections were incubated overnight at 4°C with one of the following primary antibodies: anti-NeuN (ABN78, rabbit polyclonal, Millipore, Billerica, MA; diluted 1:2000) or anti-SCGN (rabbit polyclonal Sigma-Aldrich Cat# HPA [Human Protein Atlas Number] 006641, RRID:AB_1079874, St Louis, MO; diluted 1:1000). Primary antibodies were diluted in washing buffer containing 3% normal goat serum. After incubation with the primary antibody, sections were then rinsed in buffer and incubated for 2 hr at room temperature with biotinylated goat anti-rabbit immunoglobulin G (BA1000, Vector laboratories, Burlingame, CA) diluted 1:250 in washing buffer. After several washes in buffer, sections were incubated for 1 hr at room temperature with avidin–biotin peroxidase complex (ImmunoPure ABC, Pierce, Rockford, IL; diluted 1:125). Peroxidase activity was revealed with 0.01% hydrogen peroxide, using 3,3′-diaminobenzidine (Sigma, St Louis. MO; 0.05%). Finally, sections were mounted, dehydrated and coverslipped with DEPEX (VWR, Rannor, PA). In addition, other sections were chosen for counterstaining with toluidine blue (Merck, Darmstadt, Germany) with the purpose of identifying hippocampal fields and layers, as well as other brain areas. Observations were made with a digital microscope (BX51, Olympus). Immunostaining was absent when the primary antibody was omitted. All the experimental groups were assayed in parallel.

3 | RESULTS

Since small changes visualized using immunohistochemical techniques are typically found from experiment to experiment, even using sections from the same brains, subtle changes are difficult to interpret. Thus, we were only looking for large, obvious differences between species or in different experimental conditions. Therefore, we analyzed qualitatively the pattern of immunostaining for SCGN in the different subdivisions of the head and body portions of the human hippocampus (Figures 1–5) (DG, CA1, CA2, CA3, subiculum, presubiculum, and parasubiculum) as well as in the EC and PRC cortices, according to the indications of the atlas of Mai, Majtanik, and Paxinos (2016). In rats and mice, we examined these regions from Bregma −2.04 to −6.60 (rat atlas; Paxinos & Watson, 2007) and from Bregma −0.94 to −3.88 (mouse atlas, Paxinos & Franklin, 2001), respectively, (Figures 6–10). In order to separate the different fields of the hippocampal formation and the boundaries between them, we used an antibody for NeuN, which specifically recognizes a soluble, nuclear, neural vertebrate DNA-binding protein that is present in the vast majority of mature neurons in both the central and peripheral nervous systems of several vertebrate species, including humans (Mullen, Buck, & Smith, 1992; Sarnat, Nochlin, & Born, 1998; Wolf et al., 1996).

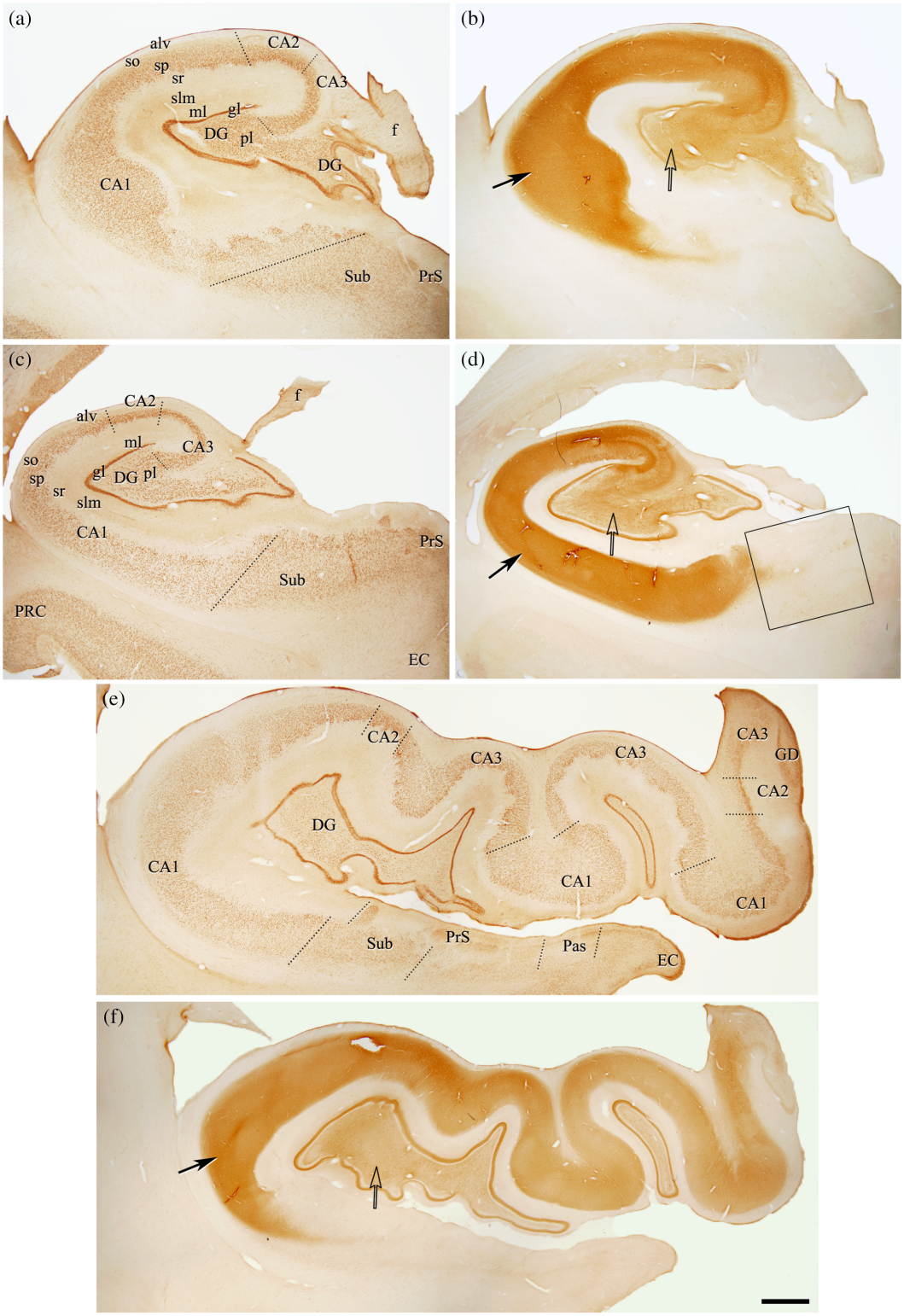

FIGURE 1 Coronal sections of the human hippocampus at the level of the hippocampal body (a–d) and the hippocampal head (e, f). Low-power photographs from sections immunostained for anti-NeuN (a, c, e) and anti-SCGN (b, d, f) from cases AB1 (a, b, e, f) and AB3 (c, d). Note the similar pattern of SCGN immunostaining in the human cases as well as in the different levels of the hippocampus (body and head). The labeled neuropil showed two types of staining (see also Figure 2): a dense brownish diffuse staining (Type I neuropil staining) (solid arrows), and a light diffuse staining (Type II neuropil staining) (open arrows). The area indicated by a rectangle in (d) is shown at a higher magnification in Figure (3d). alv, alveus; CA1–CA3, hippocampal CA fields; DG, dentate gyrus; EC, entorhinal cortex; f, fimbria; gl, granular layer; ml, molecular layer; Pas, parasubiculum; pl, polymorphic layer; PRC, perirhinal cortex; PrS, presubiculum; slm, stratum lacunosum moleculare; sp, stratum piramidale; sr, stratum radiatum; Sub, subiculum; so, stratum oriens. Scale bar shown in (f) indicates 1,460 μm in (a–d), 1,600 μm in (e), and 1,720 μm in (f) [Color figure can be viewed at wileyonlinelibrary.com]

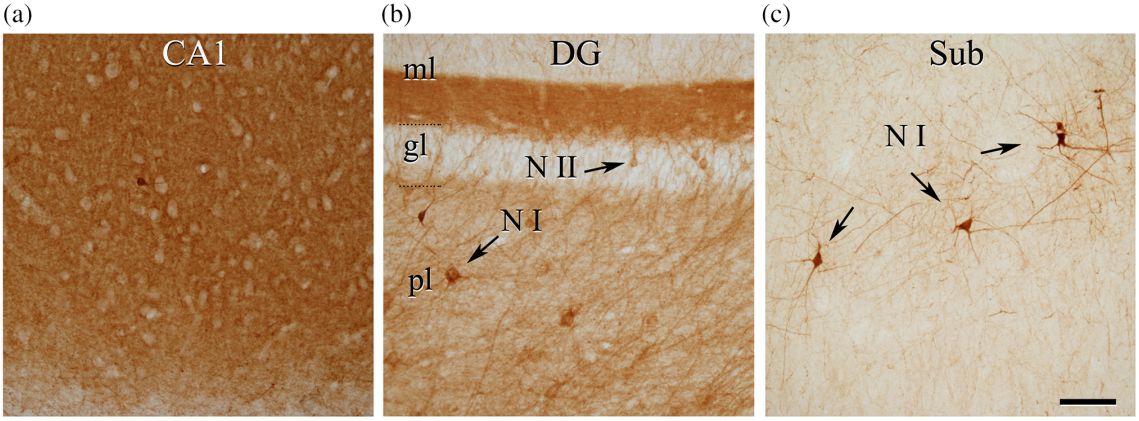

FIGURE 2 Photomicrographs from case AB3 illustrating the different patterns of SCGN immunostaining in the neuropil and neurons of the human hippocampus (a–c). (a) Shows Type I neuropil staining (dense brownish diffuse staining: no individual neuronal processes are distinguished. (b) Shows the three possible staining patterns of the neuropil; Type I neuropil staining in the inner third of the molecular layer (ml); Type II immunostaining (light diffuse staining in which scattered stained neuronal processes are observed) in the polymorphic layer (pl); and no labeling of the neuropil in the granular layer (gl) and outer upper molecular layer (ml). Some Type I (N I) and II (N II) SCGN-ir neurons are indicated (arrows). (c) Illustrates a lack of staining of the neuropil while several Type I (N I) SCGN-ir neurons are observed (arrows). Note the nonpyramidal cell morphology of the labeled cells in the subiculum (sub). CA1, CA1 field of the hippocampus; DG, dentate gyrus; gl, granular layer; ml, molecular layer; pl, polymorphic layer; Sub, subiculum. Scale bar shown in (c) indicates 90 μm in all panels [Color figure can be viewed at wileyonlinelibrary.com]

3.1 | SCGN immunostaining patterns in the hippocampal formation

The pattern of SCGN immunostaining in the human, rat, and mouse hippocampus showed numerous similarities and also clear differences between each of these species. Interestingly, some patterns of immunostaining showed a higher degree of similarity between humans and rats, whereas others had a greater degree of similarity between humans and mice.

In general, the neuropil was either labeled or not labeled. The labeled neuropil showed two types of staining: a dense brownish diffuse staining (Type I neuropil staining), in which no individual neuronal processes are distinguished (Figures 1b,d and 2b), and a light diffuse staining (Type II neuropil staining), in which scattered stained neuronal processes are observed (Figures 1b,d and 2b). We also found two main types of labeling of neurons and their proximal processes: a dark brown (Golgi-like) staining (Type I neuronal staining) (Figure 2b,c) and a light brownish staining (Type II neuronal staining) (Figure 2b). Regarding the morphology of the SCGN-ir cells, when the dendrites were clearly labeled (Type I neuronal staining), it was observed that the vast majority showed a nonpyramidal morphology (interneurons) in all species. Light labeled cells were difficult to classify as pyramidal or nonpyramidal cells, but they were considered pyramidal when their soma was a triangular shape with a vertically oriented apical dendrite emerging from it. In regions with pattern I neuropil staining, labeled neurons were absent or only occasionally found (Figure 2a). Unless otherwise specified, we will use "SCGN-ir cells" to refer to both Types I and II neurons. What follows is a description of the SCGN staining in the human, rat, and mouse.

3.1.1 | Pattern of SCGN immunostaining in the human hippocampal formation

The hippocampus, together with the EC and PRC, parahippocampal cortex, and HC, forms the medial temporal lobe system, considered pivotal to memory (Eichenbaum & Lipton, 2008; Squire & Zola-Morgan, 1991). In the head and body of the human hippocampus, the fields with SCGN immunostaining were observed in the neuropil of the pyramidal cell layer and strata oriens and radiatum of CA1, CA2, and CA3, although these three fields exhibited differences in SCGN immunostaining intensity. As shown in Figures 1–4, CA1 and CA2 show Type I neuropil staining, whereas CA3 and DG display Type II neuropil staining. There is a clear decrease in SCGN immunostaining in stratum lacunosum moleculare and alveus of CA1–CA3 and in the outer two thirds of the molecular layer of the DG. Furthermore, we observed a clear decrease in the staining of the neuropil in strata pyramidale and radiatum of CA, close to the subiculum.

The subiculum is the major output structure of the hippocampus proper, which receives a large and robust projection from CA1 and in turn sends its major projection to EC (Amaral, Dolorfo, & Alvarez-Royo, 1991; O'Mara, 2006; O'Mara, Commins, Anderson, & Gigg, 2001). The subiculum has three layers with a deep, polymorphic layer; a pyramidal cell layer containing the principal cells; and a molecular layer, which is continuous with the stratum lacunosum moleculare of field CA1 (Ding, 2013). As shown in Figures 1–4, the subiculum showed a clear decrease in staining of the neuropil, and an increase in the number of SCGN-ir cells (Figure 3d). Furthermore, we also observed this pattern of staining in presubiculum and parasubiculum. The CA1/subicular border is marked by a rather abrupt narrowing of

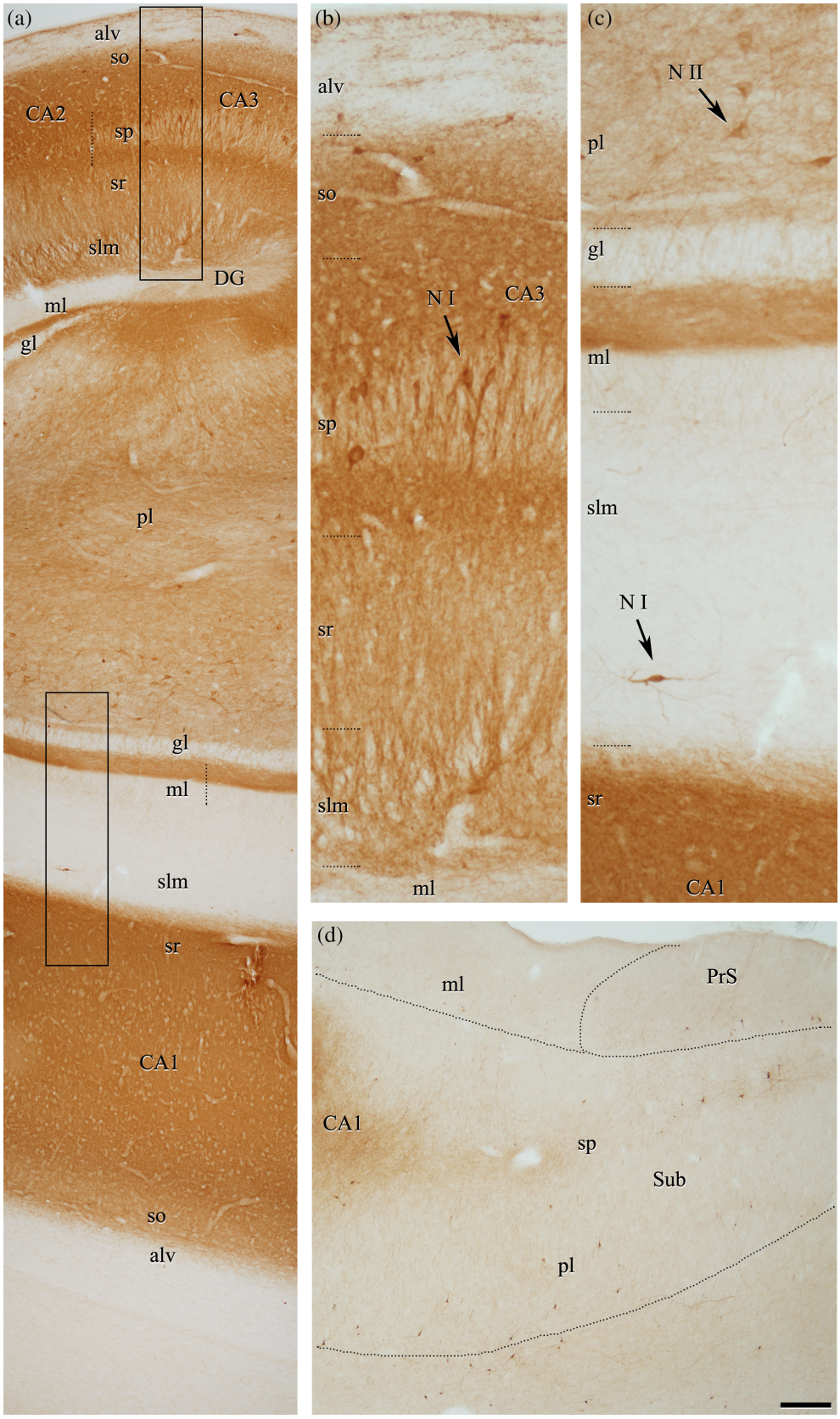

FIGURE 3 Photomicrographs from case AB3 illustrating the differences in the pattern of SCGN staining in the DG, CA1–CA3 (a–c), subiculum and presubiculum (d). Rectangles in (a) indicate the areas of magnification in (b) and (c). Note a clear decrease in SCGN immunostaining of neuropil in the alveus (alv) and in the stratum lacunosum moleculare of CA1 and granular layer (gl) of the DG. By contrast, there is an intense neuropil staining in the pyramidal cell layer in CA1, CA2, and CA3 (a–c), and in the inner third of molecular layer (ml) and polymorphic layer of the DG (c). CA1 shows very few immunostained neurons, whereas some stained neurons (arrows) are present in CA2, CA3, and DG (a–c). (d) Higher magnification of the area indicated by a rectangle in Figure 1d to show the sharp decrease in staining of the neuropil of CA1 close to the subiculum. There is also a virtual lack of immunostaining in the neuropil of the subiculum and presubiculum. alv, alveus; CA1, CA1 field of the hippocampus; CA2, CA2 field of the hippocampus; CA3, CA3 field of the hippocampus; DG, dentate gyrus; gl, granular layer; ml, molecular layer; pl, polymorphic layer; PrS, presubiculum; slm, stratum lacunosum moleculare; sp, stratum piramidale; sr, stratum radiatum; Sub, subiculum; so, stratum oriens. Scale bar shown in (d) indicates 240 μm in (a), 70 μm in (b) and (c), and 340 μm in (d) [Color figure can be viewed at wileyonlinelibrary.com]

the neuropil immunostaining of the CA1 pyramidal cell layer. In the subiculum, SCGN-ir cells were found in all layers but they were more abundant in the deep polymorphic layer. In the presubiculum, SCGN-ir cells were more numerous in Layers II–III, whereas—in the parasubiculum—SCGN-ir cells were localized in deep layers, mostly Layer V (Figure 4c,d).

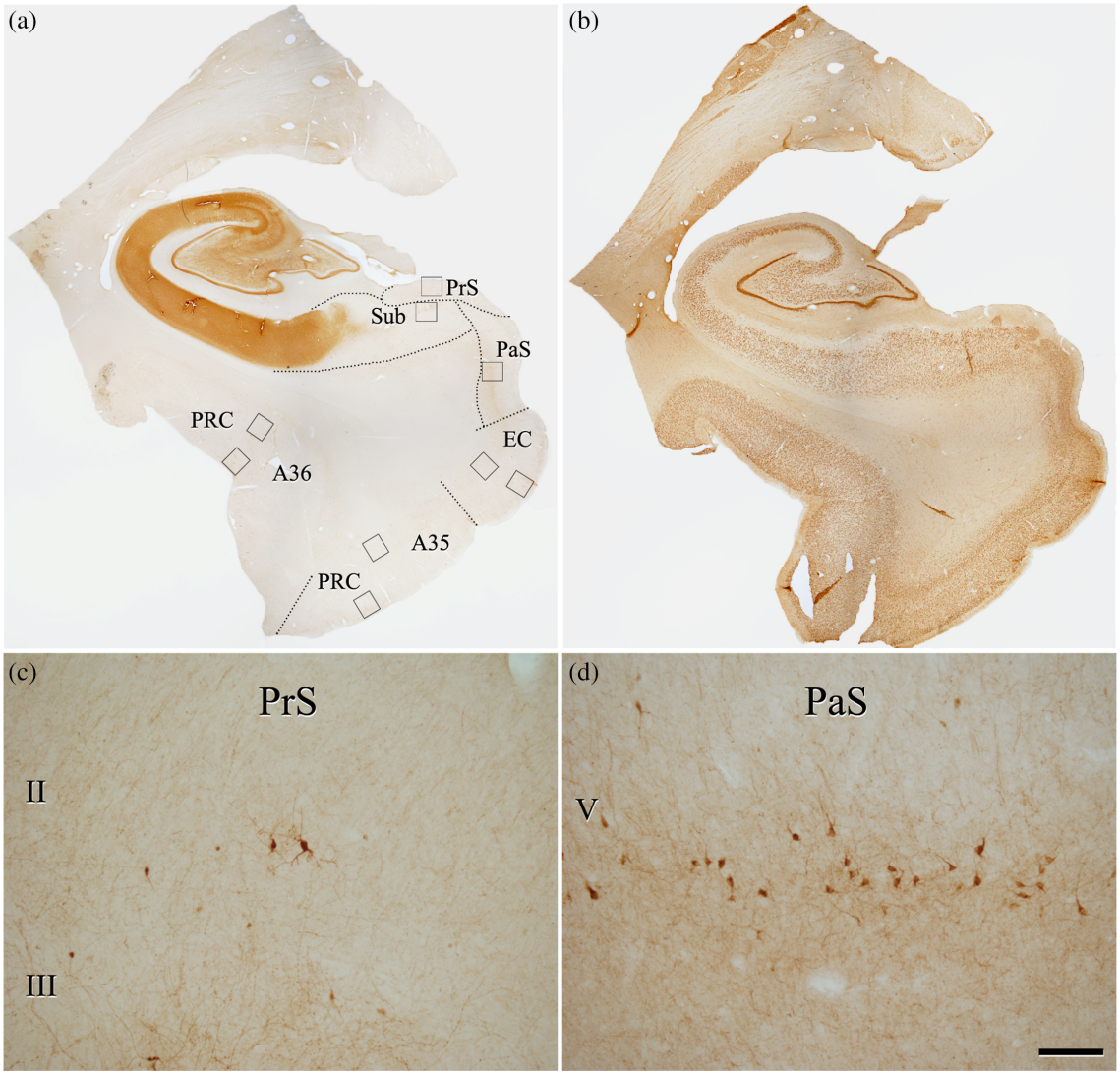

FIGURE 4 (a, b) Low-power photographs of sections stained for SCGN (a) and NeuN (b) from case AB3 and higher magnification of SCGN immunostaining of cells in the subiculum, presubiculum, and parasubiculum. Rectangles in (a) indicate the areas of magnification in (c, d) and in Figure 5. (c, d) Higher magnification photomicrographs showing Type II SCGN cells in Layers II–III of the presubiculum (c) and in layer V of the parasubiculum (d). Note the differences in the distribution of Type II SCGN-ir cells between the layers, with them being more abundant in Layers II–III in presubiculum (c) and in Layer V in parasubiculum (d). A35, area 35; A36, area 36; EC, entorhinal cortex; Pas, parasubiculum; PRC, perirhinal cortex; PrS, presubiculum; Sub, subiculum. Scale bar shown in (d) indicates 2,300 μm in (a) and (b), 100 μm in (c) and (d) [Color figure can be viewed at wileyonlinelibrary.com]

The EC is the main interface between the hippocampus and neocortex (Insausti, Amaral, & Cowan, 1987), which projects to the DG and hippocampal fields CA3 and CA1 via the perforant pathway (Kerr, Agster, Furtak, & Burwell, 2007). In the EC, most SCGN-ir cells were located in Layer II, while in Layer V these neurons were scarce (Figure 5a,d). In the PRC, which includes Brodmann's areas 35 (A35) and 36 (A36), SCGN-ir cells were located mainly in Layers II–III of A35 (Figure 5b,e) as well as in deep layers, whereas A36 showed scattered cells throughout all layers, although fewer immunoreactive cells were found in deep layers (Figure 5c,f).

3.1.2 | Pattern of SCGN immunostaining in the rat hippocampal formation

This study was carried out in the brain of animals that were either perfused or fixed by immersion after different PT delays. In hippocampus, the pattern of immunostaining in the rat hippocampal formation showed notable differences in comparison to humans. Furthermore, we found clear differences in the pattern of immunostaining between dorsal and ventral hippocampal regions. In the dorsal zone, the labeling of neurons and neuropil was found mainly in the strata lacunosum moleculare, radiatum, pyramidale, and oriens of CA1, which extended to the fasciola cinerea (Figures 6a,c,d and 7a). We observed—especially in the border of CA1 and the fasciola cinerea—a relatively large number of cell bodies and fibers in the neuropil (Figure 6a), and a decrease in labeling of the neuropil and somata, in stratum pyramidale of CA2 and CA3 (Figure 7c), and in the granular and polymorphic layers of the DG (Figure 7a). In the granular layer of DG, there were few or no Type II SCGN-ir cells in the subgranular zone (Figures 6a,c and 7a). Curiously, in the temporal extreme, the DG had relativity more SCGN-ir cells in the inner third of the molecular layer,

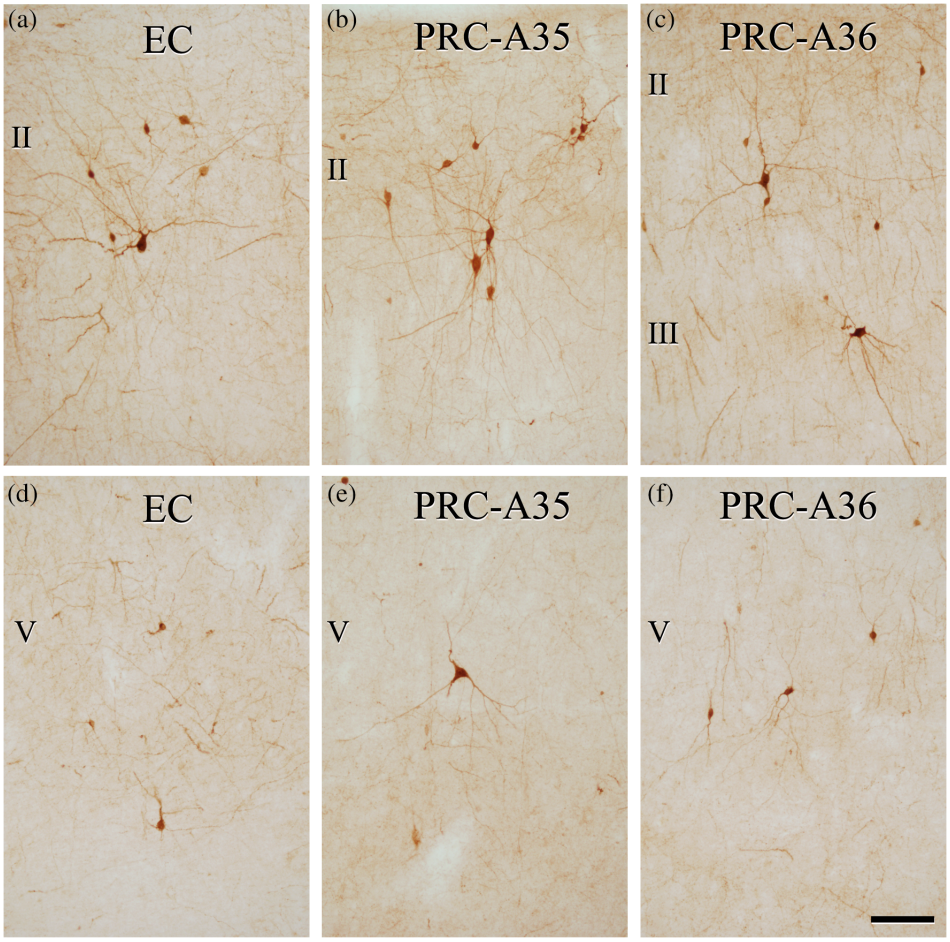

FIGURE 5 Higher magnification of the areas indicated by a rectangle in Figure 4a. (a–c) SCGN-ir cells in the upper layers of the entorhinal cortex (EC) (a); perirhinal cortex-area 35 (PRC-A35) (b); and perirhinal cortex-area 36 (PRC-A36) (c). (d–f) Labeled neurons in deep layers of EC, PRC-A35, and PRC-A36. Note the nonpyramidal cell morphology of the labeled cells. Scale bar shown in (f) indicates 90 μm in all panels [Color figure can be viewed at wileyonlinelibrary.com]

similar to human brain (Figure 6e). The hilus exhibited intense labeling in the neuropil and a relatively large number of SCGN-ir cells in the polymorphic layer of the DG. Moreover, there were fewer labeled somata in the stratum pyramidale of CA1, relative to the dorsal zone (Figure 6e). Another difference that could be observed along the dorso-ventral axis was neuropil staining of strata pyramidale, radiatum, and lacunosum moleculare of CA1, which waned gradually and faded out in the ventral part of the hippocampus (Figure 6e).

In the subiculum, pre- and parasubiculum, the SCGN immunostaining was observed mainly in cell bodies. The pyramidal cell layer of the subiculum contains deep aspects (adjacent to the alveus) and superficial aspects (adjacent to the molecular layer of the subiculum) (Drexel, Preidt, Kirchmair, & Sperk, 2011). We observed that the dorsal and ventral zones of the subiculum had different distribution patterns (Figures 6e and 8a,c,d). At the ventral subiculum (VS), a relatively large number of SCGN-ir cells were observed next to the border with the alveus (deep layer). However in the dorsal zone, the stained cells were scattered through the subiculum, and the superficial pyramidal layer had mostly Type-I SCGN-ir somata. The presubiculum only had SCGN immunostaining in the neuropil and the parasubiculum in somata (Figure 8e).

In rodents, the EC has two main classical subdivisions, namely the lateral and medial entorhinal area (LEA and MEA, respectively), with three subdivisions having been described for LEA and two for MEA (Insausti, Herrero, & Witter, 1997; van Groen, 2001). In the present work, the observations have been focused on the LEA. In this subdicision of the EC, SCGN-ir cells were mainly located in deep Layers V–VI (Figure 9c,d). In the PRC (comprising area 35 and area 36) exhibited SCGN-ir somata mainly in Layers III and V, although they were observed in other layers (Figure 9f).

Although in the present study we have focused on the hippocampal formation, as well as the EC and PRC, we observed in the rat and mouse an intense immunostaining for SCGN in other brain areas such as the superior colliculus (SC), the peripeduncular nucleus (PP) (Figure 6e), and the basolateral amygdaloid nucleus (BLP) (Figure 9a). These other brain regions were not examined in the human brain.

3.1.3 | Pattern of SCGN immunostaining in the mouse hippocampal formation

The pattern of SCGN located in the mouse hippocampus was also different compared to rat and human, although some similarities were shared between mouse and each of the other two species. Apparently, the mouse hippocampus does not show differences between the dorsal and ventral zones as pronounced as in the rat hippocampus, although our observations revealed a decrease in the intensity of labeling in all the layers of ventral hippocampus (Figure 6b,d,f).

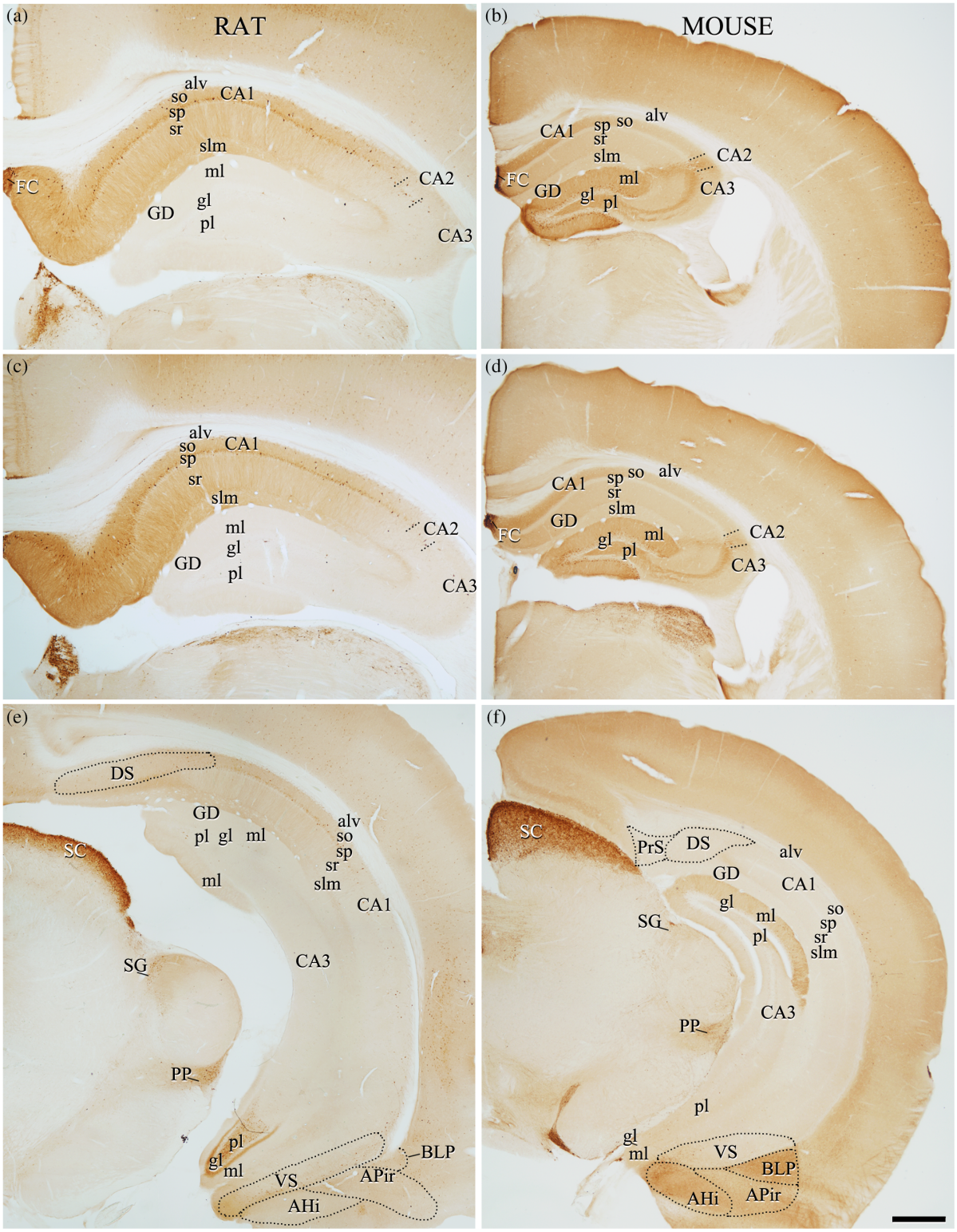

FIGURE 6 Coronal sections of the rat and mouse brain (from perfused brains). Low-magnification photomicrographs showing differences in the general pattern of SCGN immunostaining of sections from the rat (a, c, e) and mouse (b, d, f) brains. alv, alveus; AHi, amygdalohippocampal area, posteromedial part; APir, amygdalopiriform transition area; BLP, basolateral amygdaloid nucleus, posterior part; CA1, CA1 field of the hippocampus; CA2, CA2 field of the hippocampus; CA3, CA3 field of the hippocampus; DG, dentate gyrus; DS, dorsal subiculum; EC, entorhinal cortex; FC, fasciola cinerea; gl, granular layer; ml, molecular layer; Pas, parasubiculum; pl, polymorphic layer; PP, peripeduncular nucleus; PRC, perirhinal cortex; PrS, presubiculum; SC, superior colliculus; SG, supragenicular thalamic nucleus; slm, stratum lacunosum moleculare; so, stratum oriens; sp, stratum piramidale; sr, stratum radiatum; VS, ventral subiculum. Scale bar shown in (f) indicates 490 μm in (a–d) and 670 μm in (e) [Color figure can be viewed at wileyonlinelibrary.com]

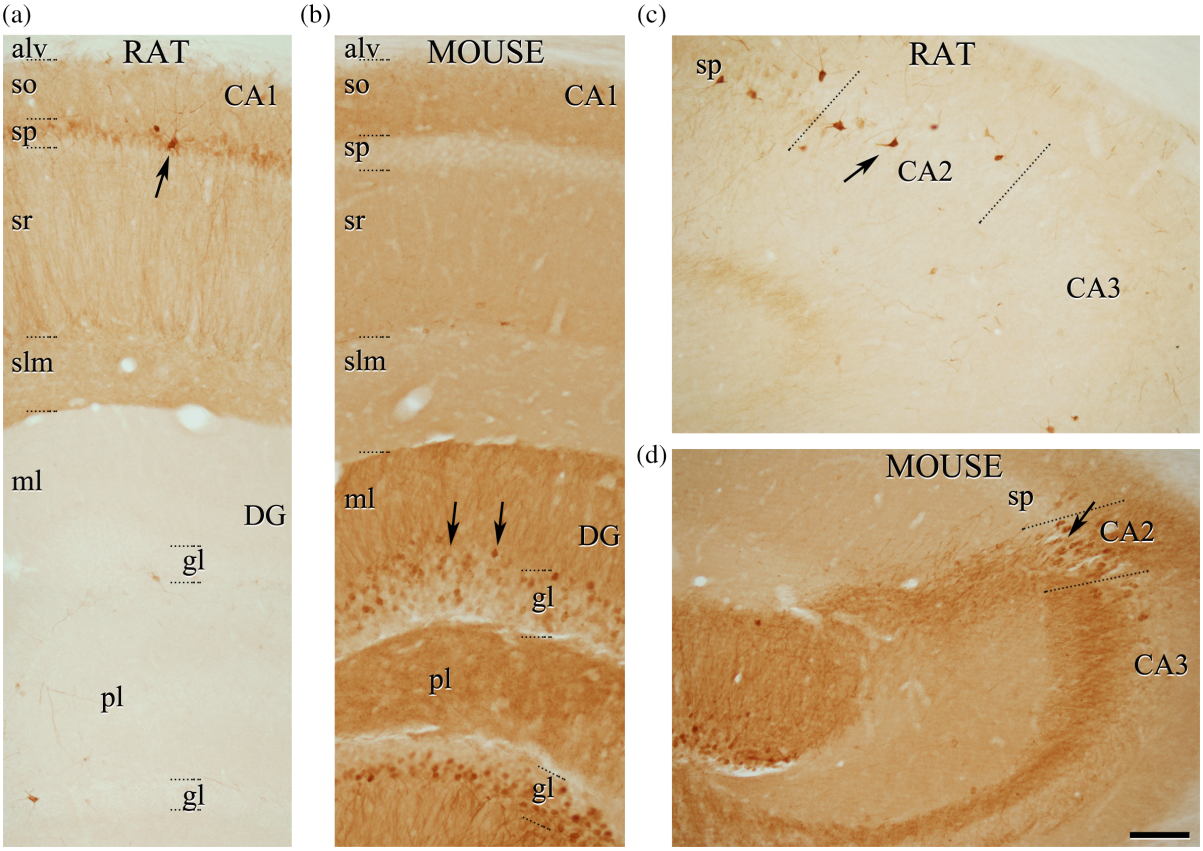

FIGURE 7 Differential pattern of SCGN immunostaining in rat (a, c) and mouse (b, d) hippocampal field (from perfused brains). Note that in the rat there are SCGN-ir cells located in the stratum pyramidale in CA1 (a) and CA2 (c) (arrows). In the mouse (b, d), there are no immunostained neurons in the stratum pyramidale of CA1 (b) but these are present in CA2 (d) (arrow). Furthermore, there is a virtual lack of immunostaining in the DG of the rat (a) in contrast to the mouse (b), where the neuropil is stained as well as the granule cells (arrows). alv, alveus; CA1, CA1 field of the hippocampus; CA2, CA2 field of the hippocampus; CA3, CA3 field of the hippocampus; DG, dentate gyrus; gl, granular layer; ml, molecular layer; pl, polymorphic layer; slm, stratum lacunosum moleculare; so, stratum oriens; sp, stratum piramidale; sr, stratum radiatum. Scale bar shown in (d) indicates 100 μm in (a, c, and d) and 70 μm in (b) [Color figure can be viewed at wileyonlinelibrary.com]

In the dorsal hippocampus, the fasciola cinerea exhibited an intense labeling in neuropil and somata (Figure 6b,d). Furthermore, it could be observed clearly that—as was the case in human hippocampus—the pyramidal cell layer of CA1 did not display cellular immunostaining, or it was weak in this layer. A similar pattern was seen in CA3, where the labeling was more intense in the neuropil, especially in mossy fibers. On the other hand, intense staining was observed in somata located in the pyramidal cell layer of CA2 and also in the neuropil consistently immunostained for SCGN (Figure 6b,d), which allowed the boundaries of CA2 to be displayed clearly (Figures 6b,d and 7d). Interestingly, this staining faded out in the ventral zone of the hippocampus. By contrast, this pattern of staining in CA2 was not present in the rat hippocampus (Figures 6a,c and 7c,d). The SCGN labeling in the neuropil was also detected in the stratum oriens of CA1 that exhibited strong SCGN staining, as well as in the strata radiatum and lacunosum moleculare, and it decreased along the dorso-ventral axis, eventually disappearing (Figure 6f). The DG displayed a darkly stained granular cell layer, particularly close to the boundary with the molecular layer. This pattern of immunostaining was different from that observed in the rat and human hippocampi (Figure 6b). The molecular cell layer was intensely immunostained in the neuropil and some scattered SCGN-ir somata were found (Figure 7b).

At ventral levels of the hippocampus, the pattern of labeling showed a decrease in the immunoreactivity—although the distribution was quite similar to the dorsal hippocampus (Figure 6f), especially in the molecular and polymorphic layers and stratum oriens. The granular layer exhibited a decrease of SCGN-ir cells compared to the septal pole. At this level, the pattern of labeling was the opposite to that found in rat ventral hippocampus (Figure 6e,f).

The subiculum, unlike the human hippocampus, displayed very few labeled cell bodies at dorsal and ventral levels (Figures 6f and 8b, f–h), although some SCGN-ir cells were found in the subiculum, and these cells were more numerous at the ventral portion of the hippocampus (Figures 6f and 8b,f). The presubiculum and parasubiculum had no Type I SCGN-ir cells, although in the presubiculum a few weakly immunostained Type II SCGN-ir cells were observed and the neuropil was also stained (Figure 8b,g–h).

Likewise, in the EC and PRC, scarce and very weakly immunostained SCGN-ir cells were detected throughout the cortical layers, showing a pronounced difference with respect to the human and rat

cortex (Figure 9b,e,g). It should be noted that some SCGN-ir somata were labeled intensely, chiefly in Layers V and VI of the somatosensorial and auditory cortices.

In other brain regions, strong immunoreactivity against SCGN was visualized; for example in the SC, the PP, the BLP, and the posteromedial part of the amygdalohippocampal area (AHi) (Figure 6f),

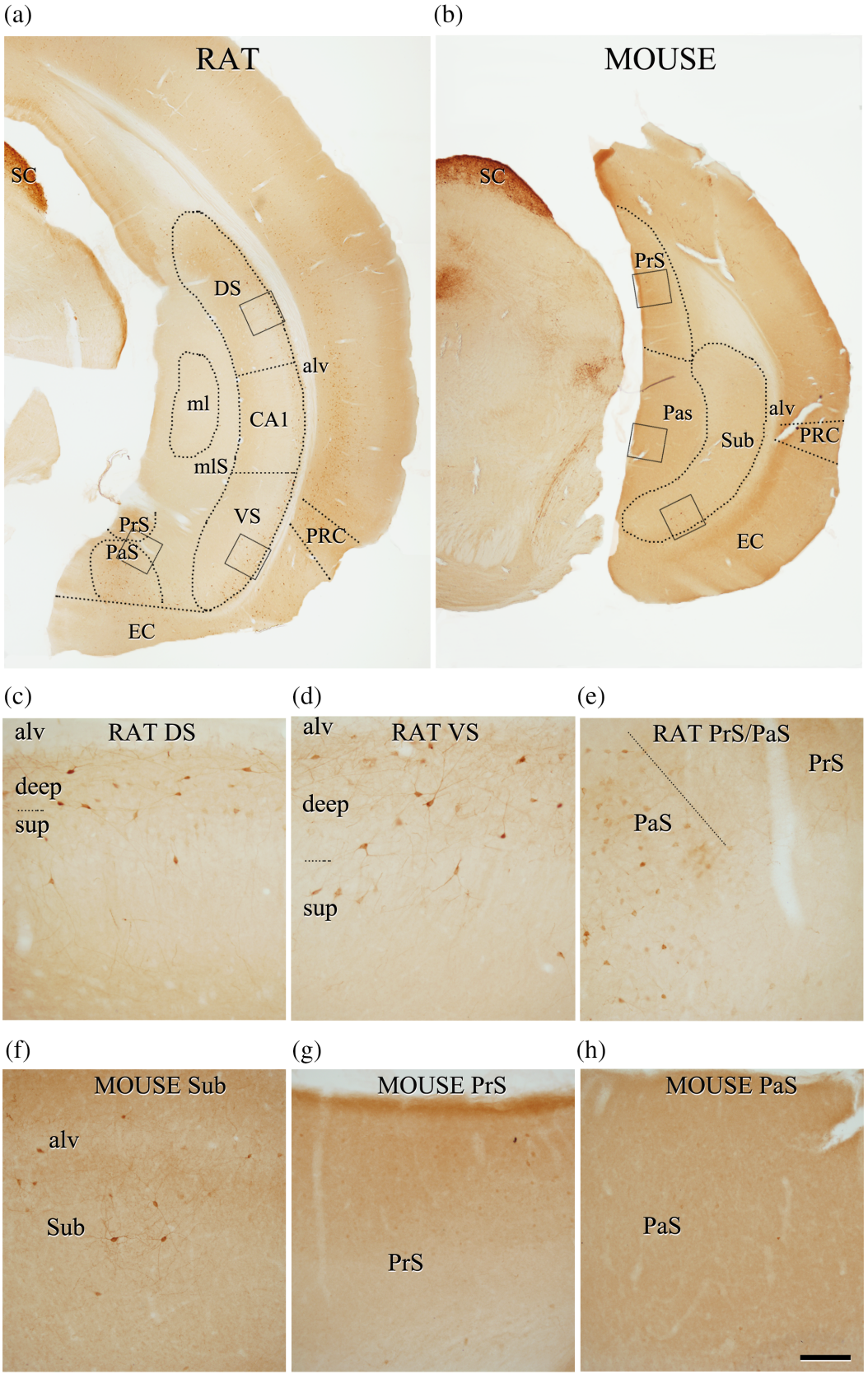

FIGURE 8 Legend on next page.

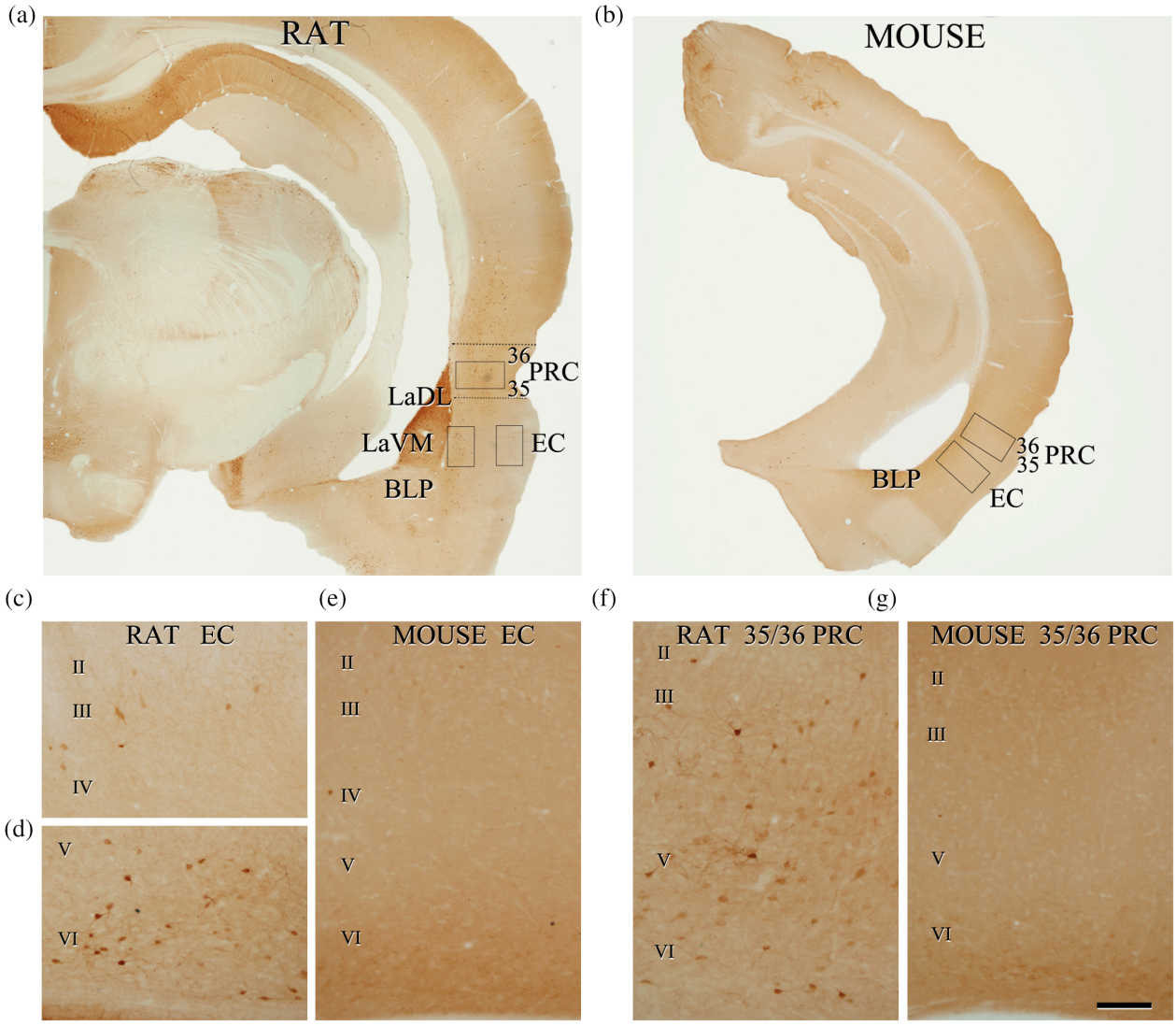

FIGURE 9 Differential distribution of SCGN immunostaining in rat and mouse brain (from perfused brains). (a, b) Low-magnification photomicrographs showing SCGN immunostaining of sections to illustrate the differential pattern of immunostaining at the level of the entorhinal and perirhinal cortices in the rat (a) and mouse (b). The areas indicated by rectangles in (a) and (b) indicate the areas of magnification in (c–g). Note that in the rat EC (c, d), SCGN-ir cells are present in all layers but they are mainly located in Layers V–VI. However, in the EC of the mouse (e), SCGN-ir cells are virtually absent. In PRC A35-A36 of the rat (f), there are SCGN-ir cells located in all layers. However, in the PRC A35-A36 of the mouse (g), very few SCGN-ir cells were present. BLP, basolateral amygdaloid nucleus, posterior part; EC, entorhinal cortex; LaDL, lateral amygdaloid nucleus, dorsolateral part; LaVM, lateral amygdaloid nucleus, ventromedial part; PRC, perirhinal cortex. Scale bar shown in (g) indicates 720 μm in (a), 570 μm in (b), and 90 μm in (c–g) [Color figure can be viewed at wileyonlinelibrary.com]

FIGURE 8 Differential distribution of SCGN immunostaining in the rat and mouse subicular complex (from perfused brains). (a, b) Low-magnification photomicrographs showing SCGN immunostaining of sections from subicular complex and neocortex of the perfused brains of rat (a) and mouse (b). The areas indicated by rectangles in (a) and (b) indicate the areas of magnification in (c–h). In (c), note the presence of scattered Types I and II SCGN-ir cells in the deep and superficial pyramidal layers of the dorsal subiculum, whereas—in the ventral subiculum—mostly SCGN-ir cells are detected, especially close to the boundary with the alveus (d). As shown in (e), the parasubiculum displays Types I and II SCGN-ir cells, whereas—in the presubiculum—there is labeling of the neuropil with few or no Type II SCGN-ir cells. Note that in the brain of mouse (b), there is an intense staining of neuropil in the subiculum, presubiculum, and parasubiculum (f–h) and few Type II SCGN-ir cells located in subiculum, especially at the ventral portion of the hippocampus (f). alv, alveus; CA1, CA1 field of the hippocampus; DS, dorsal subiculum; EC, entorhinal cortex; ml, molecular layer of the dentate gyrus; mlS, molecular layer of the subiculum; Pas, parasubiculum; pl, polymorphic layer; PRC, perirhinal cortex; PrS, presubiculum; SC, superior colliculus; Sub, subiculum; VS, ventral subiculum. Scale bar shown in (h) indicates 580 μm in (a), 460 μm in (b), 110 μm in (c–h) [Color figure can be viewed at wileyonlinelibrary.com]

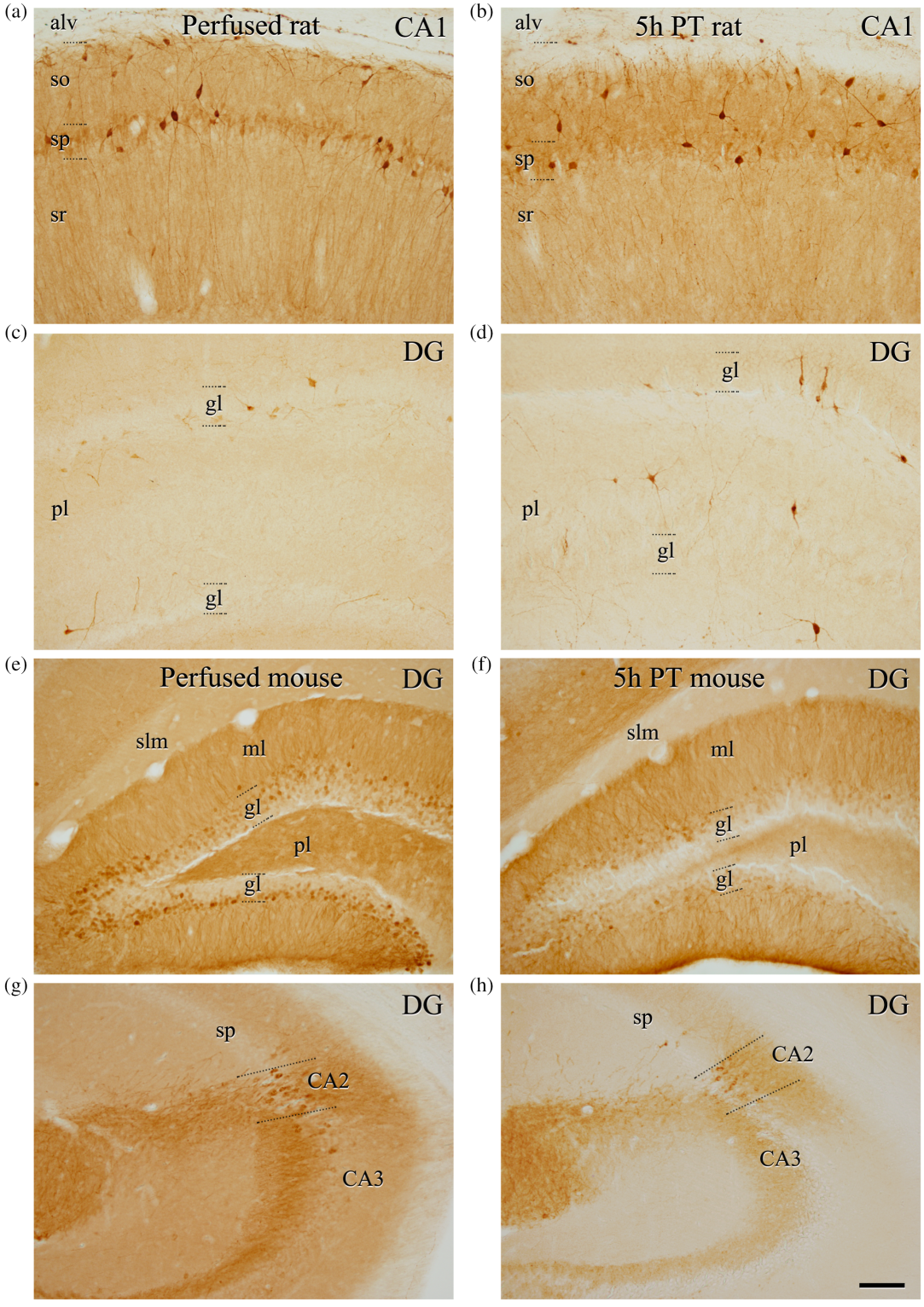

FIGURE 10 Comparison of the patterns of SCGN-immunoreactivity in the hippocampus of the rat and mouse from brains fixed by perfusion or by immersion. (a–d) Low-magnification photomicrographs showing the distribution patterns of SCGN-immunoreactivity in sections through the CA1 and DG of rat brain fixed by perfusion (a and c) or by immersion after 5 hr PT (b, d). (e–h) Low-magnification photomicrographs showing the distribution patterns of SCGN immunostaining in sections through CA1 and DG of mouse brain fixed by perfusion (e, g) or by immersion after 5 hr PT (f, h). Note the similar pattern of immunostaining obtained for the two experimental conditions (perfused vs. fixed by immersion after 5 hr PT). alv, alveus; CA1, CA1 field of the hippocampus; CA2, CA2 field of the hippocampus; CA3, CA3 field of the hippocampus; DG, dentate gyrus; gl, granular layer; ml, molecular layer; pl, polymorphic layer; slm, stratum lacunosum moleculare; so, stratum oriens; sp, stratum piramidale; sr, stratum radiatum. Scale bar shown in (h) indicates 90 μm in all panels [Color figure can be viewed at wileyonlinelibrary.com]

where, curiously, an intense neuropil staining was observed, especially in the border between VS and the posteromedial part of the amygdalohippocampal area (Figure 6f). This was not found in rat brain (Figure 6e).

3.1.4 | Pattern of SCGN immunostaining in rodent brains fixed by immersion after different post-mortem delays

We tested the possible effects of fixation by immersion after 2 and 5 hr PT delays on the immunostaining for SCGN in rat and mouse brains, as described in our previous study (Gonzalez-Riano et al., 2017). As shown in Figure 10, in general, the pattern of immunostaining was similar in brains fixed by perfusion or by immersion after up to 5 hr PT delay, in both rats (Figure 10a–d) and mice (Figure 10 e–h). The only apparent difference was a general decrease in the intensity of the labeling of Type II cells.

4 | DISCUSSION

In the present study, we have demonstrated clear differences and similarities in the pattern of SCGN immunostaining among the human, rat, and mouse hippocampal formation (DG, CA1, CA2, CA3, subiculum, presubiculum, and parasubiculum) as well as in the EC and PRC. We also found obvious differences and similarities between the different brain regions examined within each species (Tables 1–3 and Figure 11). None of these features were due to methodological factors, since the general pattern of immunostaining was similar in brains fixed by perfusion or by immersion after up to 5 hr PT delay, that is, similar to the way in which human brain tissue is obtained and processed. Importantly, the present results also indicate that PT delays of up to 5 hr do not affect the general pattern of SCGN labeling. Furthermore, some patterns were different between the human and either rat or mouse as well as between the two nonhuman species themselves. For example, the pyramidal cell layer of human CA1 (both at the level of the hippocampal body and the hippocampal head) shows an intense neuropil staining but very few SCGN-ir cells. However, regarding rat and mouse, the pyramidal cell layer of CA1 in the dorsal hippocampus showed immunostaining of both neuropil and neurons in the rat, while in the mouse the neuropil was stained but very few SCGN-ir cells were found. Furthermore, in rodents, there was a clear difference in the staining between the dorsal and ventral hippocampal formation, with a notable decrease in immunostaining in the ventral region. Another interesting example is regarding the human PrS and Pas which showed numerous SCGN-ir cells, whereas no or rarely labeled cells were found in the PrS of rat and mouse. However, SCGN-ir cells were observed in Pas of rat, but not in mouse. Finally, in the human and rat EC and PRC, there were intensely stained SCGN-ir cells (Type I cells), although the distribution patterns differed throughout the cortical layers. In the mouse EC and PRC, only occasional and weakly labeled SCGN-ir cells were observed. Regarding the morphology of the SCGN-ir cells, when the dendrites were well labeled, it was observed that the vast majority showed a nonpyramidal morphology (indicating interneurons) in all species. Light labeled cells were hard to classify as pyramidal or nonpyramidal cells, but they were considered pyramidal when their soma had a triangular shape and a vertically oriented apical dendrite emerging from it (e.g., in CA2 of the mouse and CA1 of the rat). The pattern of immunostaining that we observed in the human hippocampus is different to that observed by Attems et al. (2007). These authors examined the human hippocampus and EC and reported that both cellular and neuropil immunoreactivity were restricted to the *subiculum* and hippocampus and that, at the cellular level, only pyramidal cells in CA1–CA4 or the hilar region of the DG were stained. However, there are important methodological differences between our study and that of Attems and colleagues. They used human brain tissue with a PT interval that ranged from 6 to 18 hr; the brain tissue was fixed in 7.5% formaldehyde; they used paraffin-embedded tissue; and before immunostaining, they incubated the sections in citrate-buffer in a microwave oven (3 min, 630 W and 30 min, 240 W) (antigen retrieval). However, in our study we used human brain tissue with a PT interval ranging from 1.5 to 4 hr; the brain tissue was fixed in 4% PFA; and the brain tissue was directly cut using a vibratome and processed for immunohistochemical experiments without antigen retrieval; that is, similar to the way in which tissue is usually processed in experimental animals.

In the human hippocampus, evidence of a possible functional segregation into the anterior and posterior zones has been reported (Strange, Witter, Lein, & Moser, 2014). Briefly, in humans, memory

TABLE 1 Summary of the pattern of SCGN-immunoreactivity in the human hippocampus, subiculum, pre- and parasubiculum, EC, and PRC

Human brain area	Labeling type	
	Neuropil	Neurons
Hippocampus		
CA1	Type I: so, sp, sr Type II: alv	No or occasional labeling
CA2	Type I: so, sp, sr, slm Type II: alv	Type II: so, sp
CA3	Type I: so, sp, sr, slm Type II: alv	Types I and II: so, sp
DG	Type II: ml (inner third), pl	Type II: pl
Subiculum	No labeling	Types I and II: ml, sp, pl
Presubiculum	No labeling	Types I and II: Layers II–III
Parasubiculum	No labeling	Types I and II: Layer V
EC	No labeling	Types I and II: Layers II, V
PRC-A35	No labeling	Types I and II: Layers II, V
PRC-A36	No labeling	Types I and II: Layers II, III, V

Abbreviations: alv, alveus; CA1, CA2 and CA3 fields of the hippocampus; DG, dentate gyrus; EC, entorhinal cortex; ml, molecular layer; pl,polymorphic layer; PRC-A35, perirhinal cortex-area 35; PRC-A36, perirhinal cortex-area 36; slm, stratum lacunosum moleculare; so, stratum oriens; sp,stratum piramidale; sr, stratum radiatum.

TABLE 2 Summary of the pattern of SCGN-immunoreactivity in the rat hippocampus, subiculum, pre- and parasubiculum, EC, PRC, and other brain areas

Rat brain area	Labeling type	
	Neuropil	Neurons
Dorsal hippocampus		
CA1	Type II: so, sp, sr, slm, fc	Types I and II: so, sp
CA2	No labeling	Types I and II: so, sp
CA3	No labeling	No or occasional labeling: so, sp
DG	No labeling	Types I and II: gl, pl
Dorsal subiculum	Type II	Types I and II: deep/ superficial pcl
Ventral hippocampus		
CA1	No labeling	Types I and II: so, sp
DG	Type II: ml (inner third), pl	Types I and II: pl
Ventral subiculum	Type II	Types I and II: deep pcl
Presubiculum	Type II	No or occasional labeling
Parasubiculum	Type II	Type II
EC	Type II	Types I and II: Layers V, VI
PRC-A35	Type II	Types I and II: Layers III, V
PRC-A36	Type II	Types I and II: Layers III, V
LaDL/ LaVM	Type I	Types I and II
BLP	Type II	No or occasional labeling
APir	Type II	No or occasional labeling
AHi	No labeling	No labeling
SC	Type II	Types I and II
SG	Type II	Types I and II
PP	Type II	Types I and II

Abbreviations: AHi, amygdalohippocampal area,posteromedial part; APir, amygdalopiriform transition area; BLP, basolateral amygdaloid nucleus, posterior part; CA1, CA2 and CA3 fields of the hippocampus; DG, dentate gyrus; EC, entorhinal cortex; fc, fasciola cinerea; LaDL, lateral amygdaloid nucleus, dorsolateral part; LaVM, lateral amygdaloid nucleus; gl, granular layer; ml, molecular layer; pcl, pyramidal cell layer; pl, polymorphic layer; PRC-A35, perirhinal cortex-area 35; PRC-A36, perirhinal cortex-area 36; PP, peripeduncular nucleus; SC, superior colliculus; SG, suprageniculate thalamic nucleus; slm, stratum lacunosum moleculare; so, stratum oriens; sp, stratum piramidale; sr, stratum radiatum.

TABLE 3 Summary of the pattern of SCGN-immunoreactivity in the mouse hippocampus, subiculum, pre- and parasubiculum, EC, PRC, and other brain areas

Mouse brain area	Labeling type	
	Neuropil	Neurons
Dorsal hippocampus		
CA1	Type II: fc, so, sr, slm	No or occasional labeling
CA2	Type II: fc, so, sr, slm	Type II: sp
CA3	Type II: fc, so, sr, slm	No or occasional labeling
DG	Type I: pl, ml	Types I and II: gl
Dorsal subiculum	Type II	Type II: deep/ superficial pcl
Ventral hippocampus		
CA1	Type II	No or occasional labeling
DG	Type I: pl, ml	No labeling
Ventral subiculum	Type II	Types I and II
Presubiculum	Type I	Type II
Parasubiculum	Type I	No or occasional labeling
EC	Type I	No labeling
PRC-A35	Type I	No labeling
PRC-A36	Type I	No labeling
BLP	Type I	No labeling
APir	Type I	No labeling
AHi	Type I	No or occasional labeling
SC	Type II	Types I and II
SG	Type II	No labeling
PP	Type II	No labeling

Abbreviations: AHi, amygdalohippocampal area,posteromedial part; APir, amygdalopiriform transition area; BLP, basolateral amygdaloid nucleus, posterior part; CA1, CA2 and CA3 fields of the hippocampus; DG, dentate gyrus; EC, entorhinal cortex; fc, fasciola cinerea; gl, granular layer; ml, molecular layer; pcl, pyramidal cell layer; pl: polymorphic layer; PRC-A35, perirhinal cortex-area 35; PRC-A36, perirhinal cortex-area 36; PP: peripeduncular nucleus; SC, superior colliculus; SG, suprageniculate thalamic nucleus; slm, stratum lacunosum moleculare; so, stratum oriens; sp, stratum piramidale; sr, stratum radiatum.

systems present a double dissociation between semantic processing in the anterior hippocampus and nonsemantic processing in the posterior hippocampus (Chua, Schacter, Rand-Giovannetti, & Sperling, 2007; Giovanello, Schnyer, & Verfaellie, 2009; Strange et al., 2014). Also, in episodic memory, detailed spatial or autobiographical memory engages the posterior hippocampus (Addis, Moscovitch, Crawley, & McAndrews, 2004; Hirshhorn, Grady, Rosenbaum, Winocur, & Moscovitch, 2012). In spatial cognition, some studies have demonstrated a double dissociation in anterior versus posterior human hippocampal responses (Nadel, Hoscheidt, & Ryan, 2013; Strange, Fletcher, Henson, Friston, & Dolan, 1999). In the present study, a similar pattern of SCGN labeling was found at the level of the head and body of the human hippocampus. Therefore, the similar pattern of immunostaining along the anterior–posterior axis of the hippocampus seems to be unrelated to the functional differences between the head and body of the hippocampus.

This is in sharp contrast to the SCGN labeling in rodents, which is strong in the dorsal hippocampus and gradually decreases to the point of almost disappearing more ventrally. In the rodent brain, it has been reported that there is a functional segregation of the hippocampus into dorsal, intermediate, and ventral zones, where the dorsal hippocampus mediates cognitive functions, especially spatial memory,

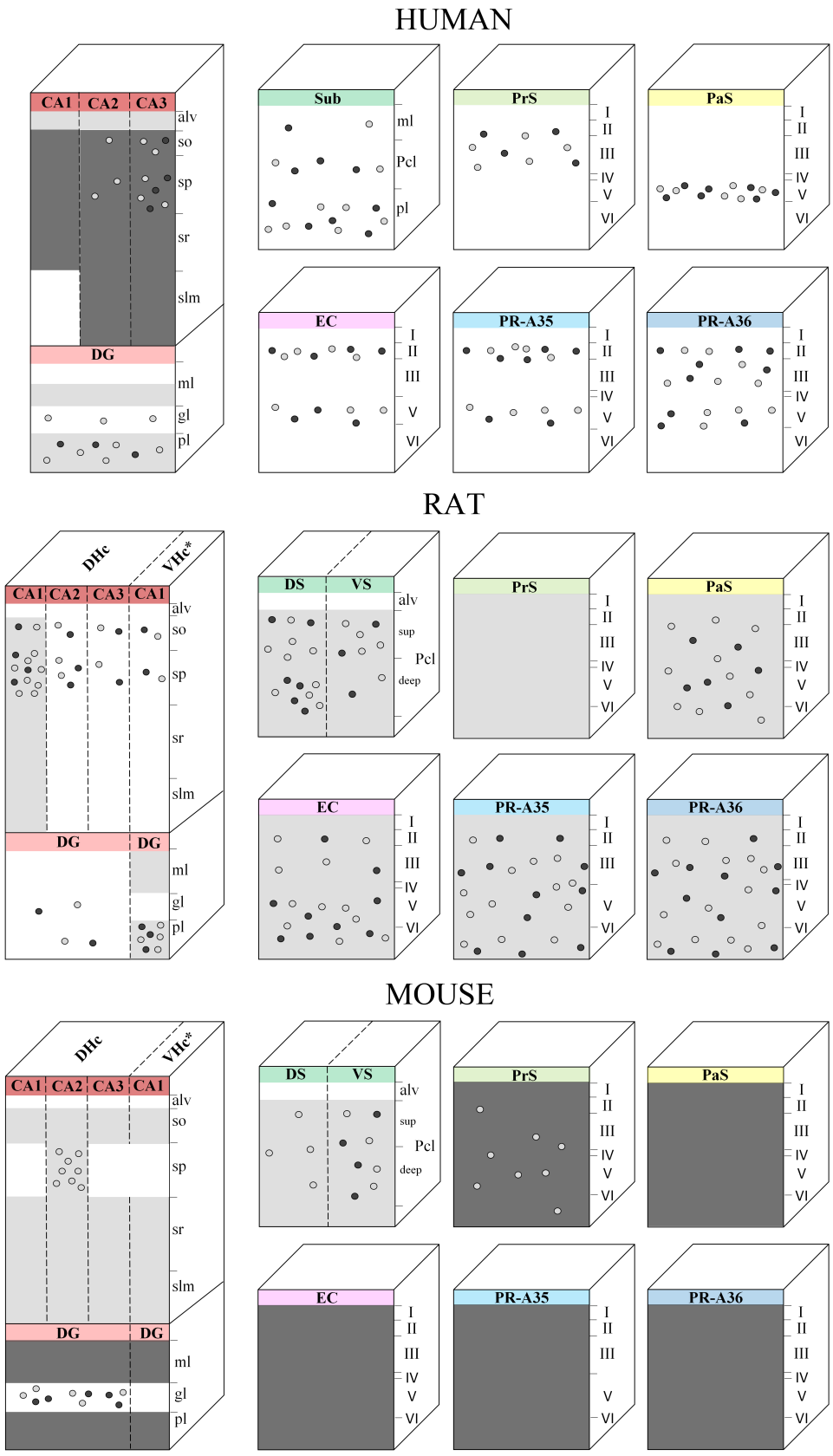

FIGURE 11 Graphical representations derived from human, rat, and mouse coronal sections, illustrating the pattern of SCGN immunostaining in neuropil and somata, through hippocampal formation (CA1, CA2, CA3, DG, subiculum, presubiculum, and parasubiculum), entorhinal (EC), and perirhinal (PRC) cortices. The areas labeled in dark gray, light gray, or white indicate Types I, II neuropil staining or no staining in neuropil, respectively. The circles in dark and light gray indicate Types I and II neuronal staining, respectively. The presence of occasional immunostained Type I or II somata are not represented in the schemes. alv, alveus; CA1, CA2, and CA3 fields of the hippocampus; DG, dentate gyrus; DHc, dorsal hippocampus; DS, dorsal subiculum; EC, entorhinal cortex; gl, granular layer; Hc, hippocampus; ml, molecular layer; Pas, parasubiculum; Pcl, pyramidal cell layer; pl, polymorphic layer; PRC-A35, perirhinal cortex-area 35; PRC-A36, perirhinal cortex-area 36; PrS, presubiculum; slm, stratum lacunosum moleculare; so, stratum oriens; sp, stratum piramidale; sr, stratum radiatum; Sub, subiculum; VHc, ventral hippocampus; VS, entral subiculum. Asterisks in VHc indicate that only CA1 is represented in the ventral hippocampus, since virtually no labeling or occasional stained cells were found in CA2, CA3, and DG. See text for further details [Color figure can be viewed at wileyonlinelibrary.com]

whereas the ventral hippocampus is involved in emotional responses (Fanselow & Dong, 2010). The ventral hippocampus seems to have a preferential role in the regulation of emotional behavior in rodents (LeDoux, 2000), and behavioral deficits correlate with the loss of hippocampal hilar neurons after kainate treatment mainly in the ventral pole of the DG (Maia et al., 2014). Since SCGN labeling is intense in

the dorsal hippocampus and almost disappears ventrally in rodents, it is tempting to speculate that this differential pattern is related to the functional segregation of the hippocampal formation. However, there are also other studies showing similarities and differences in neuronal composition between the dorsal and ventral hippocampus. For example, parvalbumin-ir neurons show no dorso-ventral difference in any subdivisions of the hippocampus, whereas the density of neurons immunostained for calretinin, nitric oxide synthase, and somatostatin is significantly larger in ventral levels than at dorsal levels of the hippocampus (Nomura et al., 1997a, 1997b).

In general, Ca^{2+}-binding proteins in the brain play important roles in the initiation and maintenance of long-term potentiation—and hence in learning and memory (Molinari et al., 1996; Schurmans et al., 1997). Although the Ca^{2+}-binding protein content does not define the main functional role of the cells, it seems that SCGN could play different roles in the modulation of cellular firing properties and the timing of the neurotransmitter released by eliminating intracellular Ca^{2+} from the cytosol (Rogstam et al., 2007). SCGN has also been related to an increase in neurite length and complexity by promoting calcium-dependent exocytosis of plasmalemmal precursor vesicles in growth cones in diverse neuronal subtypes (Raju et al., 2017). Finally, SCGN may also play a role in the regulation of the release factors related to the survival or development of new neurons in the olfactory bulb and DG (Mulder, Zilberter, et al., 2009). However, the possible significance of the dorso-ventral differences in SCGN in rodents but not in the anterior–posterior axis in humans is difficult to determine. First, there are multiple neural systems involved in the different functional attributes of the hippocampal formation and second, these systems may differ between the three species regarding cytoarchitectonic and neurochemical characteristics as well as in terms of the patterns of connectivity.

4.1 | Evaluation of post-mortem delay and fixation in rodents

The PT delay and the method of fixation are important factors to be taken into account when interpreting immunocytochemical staining. For example, previous studies in the mouse hippocampus in our laboratory described changes in immunoreactivity depending on both the PT delay and on whether parvalbumin or calbindin D-28k was used (Gonzalez-Riano et al., 2017). Since the goal in the present study was to compare between human, rat, and mouse, we investigated the possible effects of these technical factors in the mouse and rat to determine whether the possible differences in immunostaining between these species were simply methodological. We have not found apparent differences in the general pattern of SCGN staining in the mouse or rat, up to 5 hr of PT. Nevertheless, we observed a decreased intensity of the SCGN immunostaining at 2 hr PT, with this decrease becoming more evident at 5 hr PT in both species. In rat hippocampus, there was a decrease in the type II SCGN-somata (lightly labeled cells) in CA1 and CA2 and in the subgranular zone of the DG. In mouse brain there was a decrease in the labeling of type II SCGN-somata in the granular cell layer of DG. Therefore, the differences between the pattern of SCGN immunostaining in the hippocampal formation found in the present study between the human and rodents are not due to the fixation.

ACKNOWLEDGMENTS

We would like to thank Lorena Valdes and Carmen Alvarez for technical assistance, and Nick Guthrie for his excellent text editing. This work was supported by grants from the following entities: Centro de Investigación en Red sobre Enfermedades Neurodegenerativas (CIBERNED, CB06/05/0066, Spain); the Spanish "Ministerio de Ciencia, Innovación y Universidades" (grant PGC2018-094307-B-I00); and the European Union's Horizon 2020 Research and Innovation Programme under grant agreement No. 785907 (Human Brain Project, second specific grant agreement [SGA2]).

Data Availability Statement

The data that support the findings of this study are available from the corresponding author upon reasonable request.

ORCID

Silvia Tapia-González https://orcid.org/0000-0003-1616-386X
Javier DeFelipe https://orcid.org/0000-0001-5484-0660

REFERENCES

Addis, D. R., Moscovitch, M., Crawley, A. P., & McAndrews, M. P. (2004). Recollective qualities modulate hippocampal activation during autobiographical memory retrieval. *Hippocampus*, *14*(6), 752–762. https://doi.org/10.1002/hipo.10215

Amaral, D. G., Dolorfo, C., & Alvarez-Royo, P. (1991). Organization of CA1 projections to the subiculum: A PHA-L analysis in the rat. *Hippocampus*, *1*(4), 415–435. https://doi.org/10.1002/hipo.450010410

Anton-Fernandez, A., Aparicio-Torres, G., Tapia, S., DeFelipe, J., & Munoz, A. (2017). Morphometric alterations of Golgi apparatus in Alzheimer's disease are related to tau hyperphosphorylation. *Neurobiology of Disease*, *97*(Pt A), 11–23. https://doi.org/10.1016/j.nbd.2016.10.005

Archer, B. R., & Wagner, L. K. (2000). Protecting patients by training physicians in fluoroscopic radiation management. *Journal of Applied Clinical Medical Physics*, *1*(1), 32–37. https://doi.org/10.1120/1.308248

Arellano, J. I., Munoz, A., Ballesteros-Yanez, I., Sola, R. G., & DeFelipe, J. (2004). Histopathology and reorganization of chandelier cells in the human epileptic sclerotic hippocampus. *Brain*, *127*(Pt 1, 45–64.

Attems, J., Quass, M., Gartner, W., Nabokikh, A., Wagner, L., Steurer, S., … Jellinger, K. (2007). Immunoreactivity of calcium binding protein secretagogin in the human hippocampus is restricted to pyramidal neurons. *Experimental Gerontology*, *42*(3), 215–222.

Attems, J., Preusser, M., Grosinger-Quass, M., Wagner, L., Lintner, F., & Jellinger, K. (2008). Calcium-binding protein secretagogin-expressing neurones in the human hippocampus are largely resistant to neurodegeneration in Alzheimer's disease. *Neuropathology and Applied Neurobiology*, *34*(1), 23–32. https://doi.org/10.1111/j.1365-2990.2007.00854.x

Barinka, F., Salaj, M., Rybar, J., Krajcovicova, E., Kubova, H., & Druga, R. (2012). Calretinin, parvalbumin and calbindin immunoreactive interneurons in perirhinal cortex and temporal area Te3V of the rat brain:

Qualitative and quantitative analyses. *Brain Research*, *1436*, 68–80. https://doi.org/10.1016/j.brainres.2011.12.014

Cho, Y. J., Lee, J. C., Kang, B. G., An, J., Song, H. S., & Son, O. (2011). Immunohistochemical study on the expression of calcium binding proteins (calbindin-D28k, calretinin, and parvalbumin) in the cerebral cortex and in the hippocampal region of nNOS knock-out(−/−) mice. *Anatomy & Cell Biology*, *44*(2), 106–115. https://doi.org/10.5115/acb.2011.44.2.106

Chua, E. F., Schacter, D. L., Rand-Giovannetti, E., & Sperling, R. A. (2007). Evidence for a specific role of the anterior hippocampal region in successful associative encoding. *Hippocampus*, *17*(11), 1071–1080. https://doi.org/10.1002/hipo.20340

Ding, S. L. (2013). Comparative anatomy of the prosubiculum, subiculum, presubiculum, postsubiculum, and parasubiculum in human, monkey, and rodent. *The Journal of Comparative Neurology*, *521*(18), 4145–4162. https://doi.org/10.1002/cne.23416

Drexel, M., Preidt, A. P., Kirchmair, E., & Sperk, G. (2011). Parvalbumin interneurons and calretinin fibers arising from the thalamic nucleus reuniens degenerate in the subiculum after kainic acid-induced seizures. *Neuroscience*, *189*, 316–329. https://doi.org/10.1016/j.neuroscience.2011.05.021

Eichenbaum, H., & Lipton, P. A. (2008). Towards a functional organization of the medial temporal lobe memory system: Role of the parahippocampal and medial entorhinal cortical areas. *Hippocampus*, *18*(12), 1314–1324. https://doi.org/10.1002/hipo.20500

Ellis, J. K., Sorrells, S. F., Mikhailova, S., Chavali, M., Chang, S., & Sabeur, K. (2019). Ferret brain possesses young interneuron collections equivalent to human postnatal migratory streams. *The Journal of Comparative Neurology*, 1-17. https://doi.org/10.1002/cne.24711

Fanselow, M. S., & Dong, H. W. (2010). Are the dorsal and ventral hippocampus functionally distinct structures? *Neuron*, *65*(1), 7–19. https://doi.org/10.1016/j.neuron.2009.11.031

Garas, F. N., Shah, R. S., Kormann, E., Doig, N. M., Vinciati, F., & Nakamura, K. C. (2016). Secretagogin expression delineates functionally-specialized populations of striatal parvalbumin-containing interneurons. *eLife*, *5*, 1-36. https://doi.org/10.7554/eLife.16088

Gartner, W., Lang, W., Leutmetzer, F., Domanovits, H., Waldhausl, W., & Wagner, L. (2001). Cerebral expression and serum detectability of secretagogin, a recently cloned EF-hand Ca(2+)-binding protein. *Cerebral Cortex*, *11*(12), 1161–1169.

Giovanello, K. S., Schnyer, D., & Verfaellie, M. (2009). Distinct hippocampal regions make unique contributions to relational memory. *Hippocampus*, *19*(2), 111–117. https://doi.org/10.1002/hipo.20491

Gonzalez-Riano, C., Tapia-Gonzalez, S., Garcia, A., Munoz, A., DeFelipe, J., & Barbas, C. (2017). Metabolomics and neuroanatomical evaluation of post-mortem changes in the hippocampus. *Brain Structure & Function*, *222*(6), 2831–2853. https://doi.org/10.1007/s00429-017-1375-5

Hirshhorn, M., Grady, C., Rosenbaum, R. S., Winocur, G., & Moscovitch, M. (2012). Brain regions involved in the retrieval of spatial and episodic details associated with a familiar environment: An fMRI study. *Neuropsychologia*, *50*(13), 3094–3106. https://doi.org/10.1016/j.neuropsychologia.2012.08.008

Insausti, R., Amaral, D. G., & Cowan, W. M. (1987). The entorhinal cortex of the monkey: II. Cortical afferents. *The Journal of Comparative Neurology*, *264*(3), 356–395. https://doi.org/10.1002/cne.902640306

Insausti, R., Herrero, M. T., & Witter, M. P. (1997). Entorhinal cortex of the rat: Cytoarchitectonic subdivisions and the origin and distribution of cortical efferents. *Hippocampus*, *7*(2), 146–183. https://doi.org/10.1002/(SICI)1098-1063(1997)7:2<146::AID-HIPO4>3.0.CO;2-L

Kerr, K. M., Agster, K. L., Furtak, S. C., & Burwell, R. D. (2007). Functional neuroanatomy of the parahippocampal region: The lateral and medial entorhinal areas. *Hippocampus*, *17*(9), 697–708. https://doi.org/10.1002/hipo.20315

Kosaka, K., & Kosaka, T. (2013). Secretagogin-containing neurons in the mouse main olfactory bulb. *Neuroscience Research*, *77*(1–2), 16–32. https://doi.org/10.1016/j.neures.2013.08.006

Kosaka, T., & Kosaka, K. (2018). Calcium-binding protein, secretagogin, specifies the microcellular tegmental nucleus and intermediate and ventral parts of the cuneiform nucleus of the mouse and rat. *Neuroscience Research*, *134*, 30–38. https://doi.org/10.1016/j.neures.2018.01.005

Lavenex, P., Lavenex, P. B., Bennett, J. L., & Amaral, D. G. (2009). Postmortem changes in the neuroanatomical characteristics of the primate brain: Hippocampal formation. *The Journal of Comparative Neurology*, *512*(1), 27–51. https://doi.org/10.1002/cne.21906

LeDoux, J. E. (2000). Emotion circuits in the brain. *Annual Review of Neuroscience*, *23*, 155–184. https://doi.org/10.1146/annurev.neuro.23.1.155

Mai, J., Majtanik, M., & Paxinos, G. (2016). *Atlas of the human brain* (4th ed.). San Diego, CA: Academic Press.

Maia, G. H., Quesado, J. L., Soares, J. I., do Carmo, J. M., Andrade, P. A., & Andrade, J. P. (2014). Loss of hippocampal neurons after kainate treatment correlates with behavioral deficits. *PLoS One*, *9*(1), e84722. https://doi.org/10.1371/journal.pone.0084722PONE-D-13-26456 pii.

Miettinen, M., Pitkanen, A., & Miettinen, R. (1997). Distribution of calretinin-immunoreactivity in the rat entorhinal cortex: Coexistence with GABA. *The Journal of Comparative Neurology*, *378*(3), 363–378. https://doi.org/10.1002/(SICI)1096-9861(19970217)378:3<363::AID-CNE5>3.0.CO;2-1 [pii].

Molinari, S., Battini, R., Ferrari, S., Pozzi, L., Killcross, A. S., & Robbins, T. W. (1996). Deficits in memory and hippocampal long-term potentiation in mice with reduced calbindin D28K expression. *Proceedings of the National Academy of Sciences of the United States of America*, *93*(15), 8028–8033.

Mulder, J., Bjorling, E., Jonasson, K., Wernerus, H., Hober, S., & Hokfelt, T. (2009). Tissue profiling of the mammalian central nervous system using human antibody-based proteomics. *Molecular & Cellular Proteomics*, *8*(7), 1612–1622. https://doi.org/10.1074/mcp.M800539-MCP200

Mulder, J., Spence, L., Tortoriello, G., Dinieri, J. A., Uhlen, M., & Shui, B. (2010). Secretagogin is a Ca2+−binding protein identifying prospective extended amygdala neurons in the developing mammalian telencephalon. *The European Journal of Neuroscience*, *31*(12), 2166–2177. https://doi.org/10.1111/j.1460-9568.2010.07275.x

Mulder, J., Zilberter, M., Spence, L., Tortoriello, G., Uhlen, M., & Yanagawa, Y. (2009). Secretagogin is a Ca2+−binding protein specifying subpopulations of telencephalic neurons. *Proceedings of the National Academy of Sciences of the United States of America*, *106*(52), 22492–22497. https://doi.org/10.1073/pnas.0912484106

Mullen, R. J., Buck, C. R., & Smith, A. M. (1992). NeuN, a neuronal specific nuclear protein in vertebrates. *Development*, *116*(1), 201–211.

Nadel, L., Hoscheidt, S., & Ryan, L. R. (2013). Spatial cognition and the hippocampus: The anterior-posterior axis. *Journal of Cognitive Neuroscience*, *25*(1), 22–28. https://doi.org/10.1162/jocn_a_00313

Nomura, T., Fukuda, T., Aika, Y., Heizmann, C. W., Emson, P. C., & Kobayashi, T. (1997a). Distribution of nonprincipal neurons in the rat hippocampus, with special reference to their dorsoventral difference. *Brain Research*, *751*(1), 64–80 doi:S0006-8993(96)01395-9 [pii].

Nomura, T., Fukuda, T., Aika, Y., Heizmann, C. W., Emson, P. C., & Kobayashi, T. (1997b). Laminar distribution of non-principal neurons in the rat hippocampus, with special reference to their compositional difference among layers. *Brain Research*, *764*(1–2), 197–204 doi:S0006-8993(97)00457-5 [pii].

O'Mara, S. (2006). Controlling hippocampal output: The central role of subiculum in hippocampal information processing. *Behavioural Brain Research*, *174*(2), 304–312. https://doi.org/10.1016/j.bbr.2006.08.018

O'Mara, S. M., Commins, S., Anderson, M., & Gigg, J. (2001). The subiculum: A review of form, physiology and function. *Progress in Neurobiology*, *64*(2), 129–155 doi:S0301-0082(00)00054-X [pii].

Paxinos, G., & Franklin, K. (2001). *The mouse brain in stereotaxic coordinates*. San Diego, CA: Academic Press.

Paxinos, G., & Watson, C. (2007). *The rat brain in stereotaxic coordinates* (6th ed.). San Diego, CA: Academic Press.

Raju, C. S., Spatazza, J., Stanco, A., Larimer, P., Sorrells, S. F., & Kelley, K. W. (2017). Secretagogin is expressed by developing neocortical GABAergic neurons in humans but not mice and increases neurite arbor size and complexity. *Cerebral Cortex*, *28*(6):1946-1958. https://doi.org/10.1093/cercor/bhx101

Rogstam, A., Linse, S., Lindqvist, A., James, P., Wagner, L., & Berggard, T. (2007). Binding of calcium ions and SNAP-25 to the hexa EF-hand protein secretagogin. *The Biochemical Journal*, *401*(1), 353–363. https://doi.org/10.1042/BJ20060918

Sanagavarapu, K., Weiffert, T., Ni Mhurchu, N., O'Connell, D., & Linse, S. (2016). Calcium binding and Disulfide bonds regulate the stability of Secretagogin towards thermal and urea denaturation. *PLoS One*, *11* (11), e0165709.

Sarnat, H. B., Nochlin, D., & Born, D. E. (1998). Neuronal nuclear antigen (NeuN): A marker of neuronal maturation in early human fetal nervous system. *Brain Dev*, *20*(2), 88–94 doi:S0387760497001113 [pii].

Seress, L., Gulyas, A. I., Ferrer, I., Tunon, T., Soriano, E., & Freund, T. F. (1993). Distribution, morphological features, and synaptic connections of parvalbumin- and calbindin D28k-immunoreactive neurons in the human hippocampal formation. *The Journal of Comparative Neurology*, *337*(2), 208–230. https://doi.org/10.1002/cne.903370204

Schurmans, S., Schiffmann, S. N., Gurden, H., Lemaire, M., Lipp, H. P., & Schwam, V. (1997). Impaired long-term potentiation induction in dentate gyrus of calretinin-deficient mice. *Proceedings of the National Academy of Sciences of the United States of America*, *94*(19), 10415–10420.

Squire, L. R., & Zola-Morgan, S. (1991). The medial temporal lobe memory system. *Science*, *253*(5026), 1380–1386.

Strange, B. A., Fletcher, P. C., Henson, R. N., Friston, K. J., & Dolan, R. J. (1999). Segregating the functions of human hippocampus. *Proceedings of the National Academy of Sciences of the United States of America*, *96* (7), 4034–4039.

Strange, B. A., Witter, M. P., Lein, E. S., & Moser, E. I. (2014). Functional organization of the hippocampal longitudinal axis. *Nature Reviews. Neuroscience*, *15*(10), 655–669. https://doi.org/10.1038/nrn3785

van Groen, T. (2001). Entorhinal cortex of the mouse: Cytoarchitectonical organization. *Hippocampus*, *11*(4), 397–407. https://doi.org/10.1002/hipo.1054

Wagner, L., Oliyarnyk, O., Gartner, W., Nowotny, P., Groeger, M., & Kaserer, K. (2000). Cloning and expression of secretagogin, a novel neuroendocrine- and pancreatic islet of Langerhans-specific Ca2+−binding protein. *The Journal of Biological Chemistry*, *275*(32), 24740–24751. https://doi.org/10.1074/jbc.M001974200M001974200 pii.

Wolf, H. K., Buslei, R., Schmidt-Kastner, R., Schmidt-Kastner, P. K., Pietsch, T., & Wiestler, O. D. (1996). NeuN: A useful neuronal marker for diagnostic histopathology. *The Journal of Histochemistry and Cytochemistry*, *44*(10), 1167–1171.

Wouterlood, F. G., van Denderen, J. C., van Haeften, T., & Witter, M. P. (2000). Calretinin in the entorhinal cortex of the rat: Distribution, morphology, ultrastructure of neurons, and co-localization with gamma-aminobutyric acid and parvalbumin. *The Journal of Comparative Neurology*, *425*(2), 177–192. https://doi.org/10.1002/1096-9861(20000918)425:2<177::AID-CNE2>3.0.CO;2-G [pii].

How to cite this article: Tapia-González S, Insausti R, DeFelipe J. Differential expression of secretagogin immunostaining in the hippocampal formation and the entorhinal and perirhinal cortices of humans, rats, and mice. *J Comp Neurol*. 2020;528:523–541. https://doi.org/10.1002/cne.24773